

Electrostatic precipitators use electrostatic forces to collect charged particles for air cleaning and aerosol sampling. Therefore, the particle charging and The deposition of charged aerosols are required separately. Usually, two stage Precipitators are utilized and they have separate sections of charging and precipitation (or deposition). In a single stage precipitator the corona wires are in the precipitation section and the same field that creates the corona for aerosol charging also causes the precipitation. Normally, the particle charging for the precipitators is done by field charging that reaches the saturation charge.

The charged aerosol flows through an electric-field oriented perpendicular to the direction of flow and to the collection plate. For a laminar flow precipitator, particle collection can be easily estimated from the fact that

All the particles satisfying $V_{TE} > HV_x/L$ will be collected.



Center for Nano Particle Control

Seoul National U., Mechanical & Aerospace Eng.

In air-cleaning electrostatic precipitators, the flow is usually turbulent. Consider the wire-and-tube geometry shown in cross section in Fig.15.7. In a period dt that is brief compared with that required for turbulent mixing, all particles within a distance $V_{TE} dt$ of the tube wall be removed. For simplicity, we assume that particles stick if they touch the wall and are not reentrained. The fraction of particles removed during this period, dN/N , is the negative ratio of the area of the annulus,

$2\pi R V_{TE} dt$, to the total cross-sectional area of the tube, πR^2 , and is given by

$$\frac{dN}{N} = - \frac{2\pi R V_{TE} dt}{\pi R^2} = - \frac{2V_{TE} dt}{R} \quad (15.34)$$

This equation can be integrated to obtain the number concentration after a time t .

$$\int_{N_0}^{N(t)} \frac{dN}{N} = \int_0^t \frac{-2V_{TE} dt}{R} \quad (15.35)$$



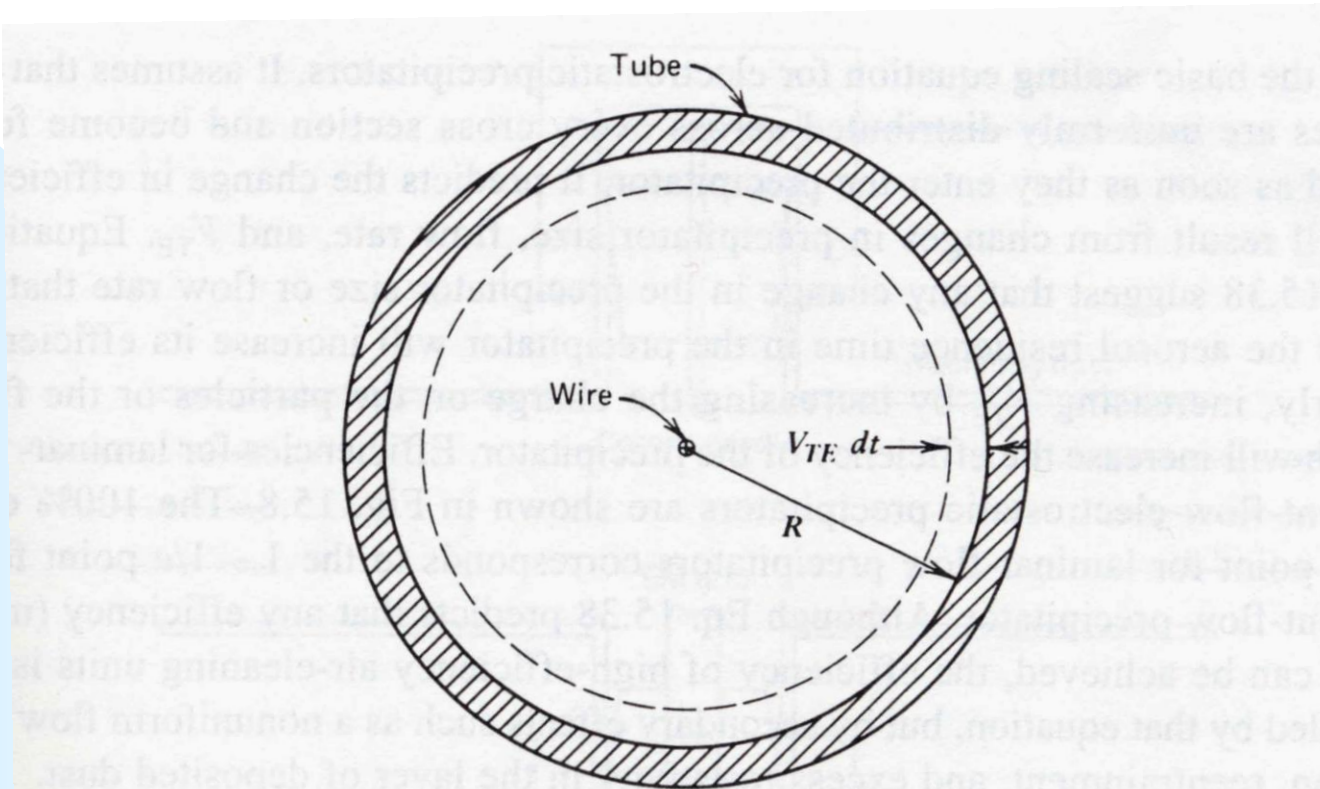


FIGURE 15.7 Cross section of a wire-and-tube electrostatic precipitator.



Center for Nano Particle Control

Seoul National U., Mechanical & Aerospace Eng.

$$\frac{N(t)}{N_0} = \exp\left(\frac{-2V_{TE}t}{R}\right) \quad (15.36)$$

For a tube of length L and volumetric flow rate Q , the residence time in the tube, $\pi R^2 L / Q$ can be substituted into Eq. 15.36 to get the penetration

– the fraction of the inlet concentration that exits the tube:

$$P = \frac{N_{out}}{N_0} = \exp\left(\frac{-2\pi V_{TE}RL}{Q}\right) \quad (15.37)$$

It is customary to express Eq. 15.37 in terms of collection efficiency and the area of the collection surface, $A_c = 2\pi RL$. Doing so gives the Deutsch–Anderson equation,



Center for Nano Particle Control

Seoul National U., Mechanical & Aerospace Eng.

$$E = 1 - \exp\left(\frac{-V_{TE} A_c}{Q}\right) \quad (15.38)$$

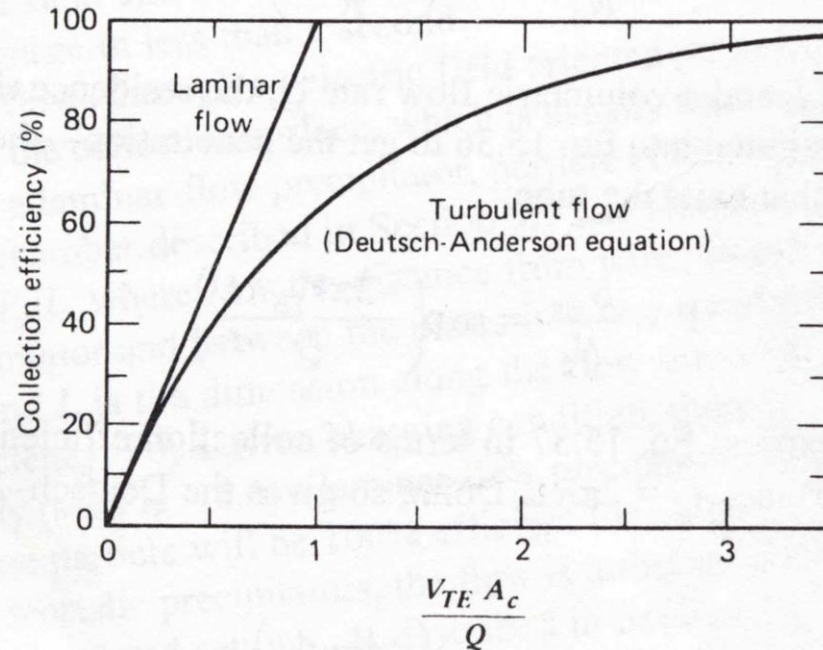


FIGURE 15.8 Efficiency curves for laminar- and turbulent-flow electrostatic precipitators.



Center for Nano Particle Control

Seoul National U., Mechanical & Aerospace Eng.

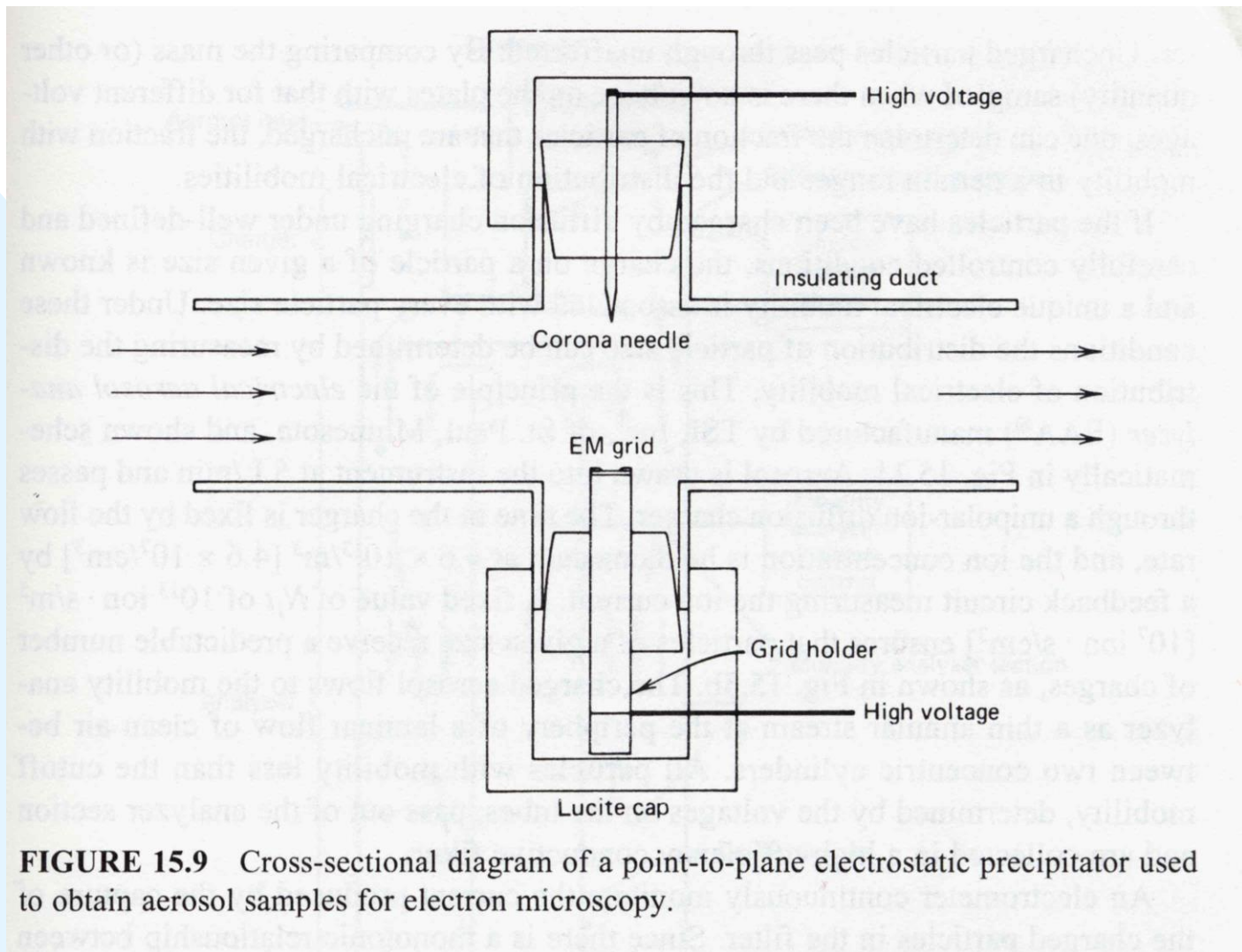


FIGURE 15.9 Cross-sectional diagram of a point-to-plane electrostatic precipitator used to obtain aerosol samples for electron microscopy.



Center for Nano Particle Control

Seoul National U., Mechanical & Aerospace Eng.

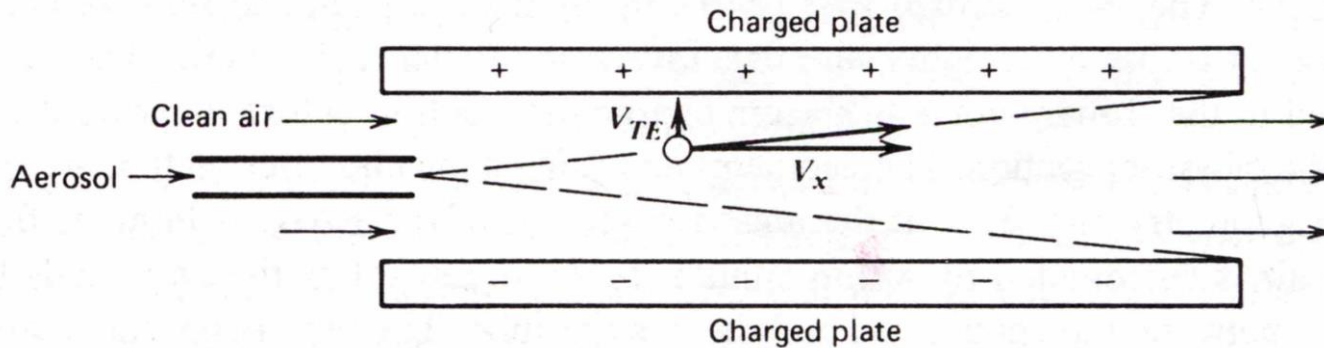


FIGURE 15.10 Diagram of a simple electrical mobility analyzer.

Aerosol particles are introduced along the centerline between two oppositely charged parallel plates. For a given voltage, all particles with mobility greater than a certain amount will migrate to the plates and be trapped. Those with lower mobility will get through to be collected on the downstream filter. Uncharged particles pass through unaffected. By comparing the mass (or other quantity) sampled when there is no voltage on the plates with that for different voltages, one can determine the fraction of particles that are uncharged, the fraction with mobility in a certain range, and the distribution of electrical mobilities.



Center for Nano Particle Control

Seoul National U., Mechanical & Aerospace Eng.

If the particles have been charged by diffusion charging under well defined and carefully controlled conditions, the charge on a particle of a given size is known and a unique electrical mobility is associated with every particle size. Under these conditions the distribution of particle size can be determined by measuring the distribution of electrical mobility. This is the principle of the electrical aerosol analyzer(EAA), TSI.

Aerosol is drawn into the instrument at 5lpm and passes through unipolar-ion diffusion charger. The time in the charger is fixed by the flow rate and ion concentration is held fixed at $4.6 \times 10^{13} / m^{+3}$ by a feedback circuit measuring the ion current. A fixed value of $NiXt$ of $10^{13} \text{ ion.s/m}^{+3}$ ensures the particles of a given size receive a predictable number of charges. The charged aerosol flows to the mobility analyzer as a thin annular stream at the periphery of a lamina flow of clean air between two concentric cylinders. All particles with mobility less than the cutoff mobility, determined by the voltage on the tubes, pass out of the analyzer section and are collected in a high efficient conductive filter. An electrometer monitors the current in the filter. Since there is a relationship between mobility and the particle size, the difference in current measured at two analyzer voltage settings is related to the number of particles in the size(mobility) range defined by the cutoff sizes of two voltage settings. This equipment measures the size distribution from 3 nm to a few hundred nanometers.

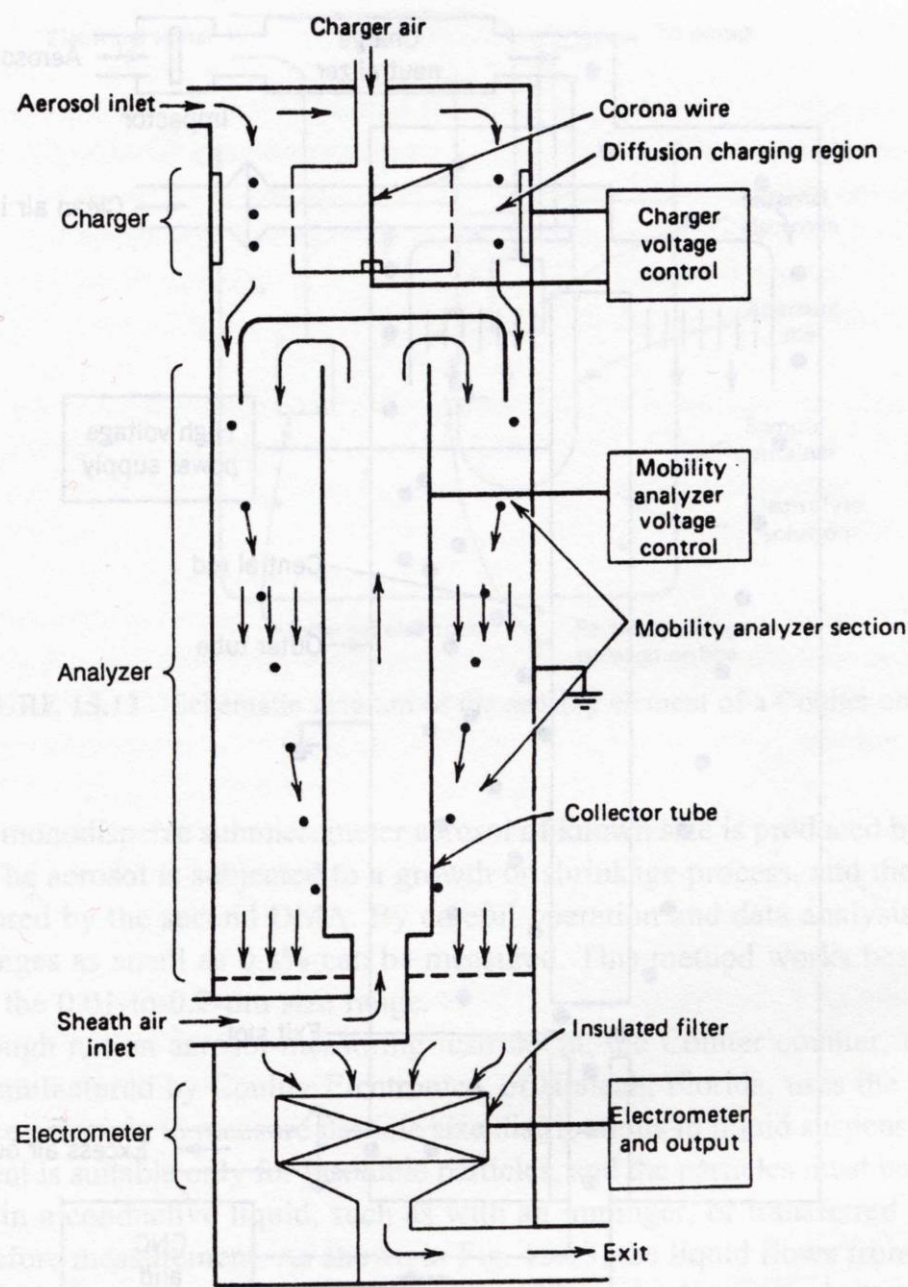


FIGURE 15.11 Schematic diagram of an electrical aerosol analyzer.



The input aerosol first passes through an impactor to remove particles larger than 10 μm . The aerosol is then neutralized to the Boltzmann equilibrium charge distribution. A laminar flow of clean air is surrounded by a thin annular layer of aerosol. The tube is grounded and the voltage on the central rod controlled between 20 and 10000V. Near the bottom of the central rod is a gap that allows a small airflow to leave the classifier and exit through a central tube. Only particles with a narrow range of mobilities can enter the gap. Particles with greater mobility migrate to the central rod before reaching the gap while those with lower mobility go beyond the gap and are filtered out. The exiting aerosol is nearly all singly charged and nearly monodisperse. Its size is controlled by adjusting the voltage on the central rod. DMA thus can classify the particle sizes and if concentration measurements system such as CNC (Condensation nucleus counter) is combined in the downstream, it can measure the size distributions.

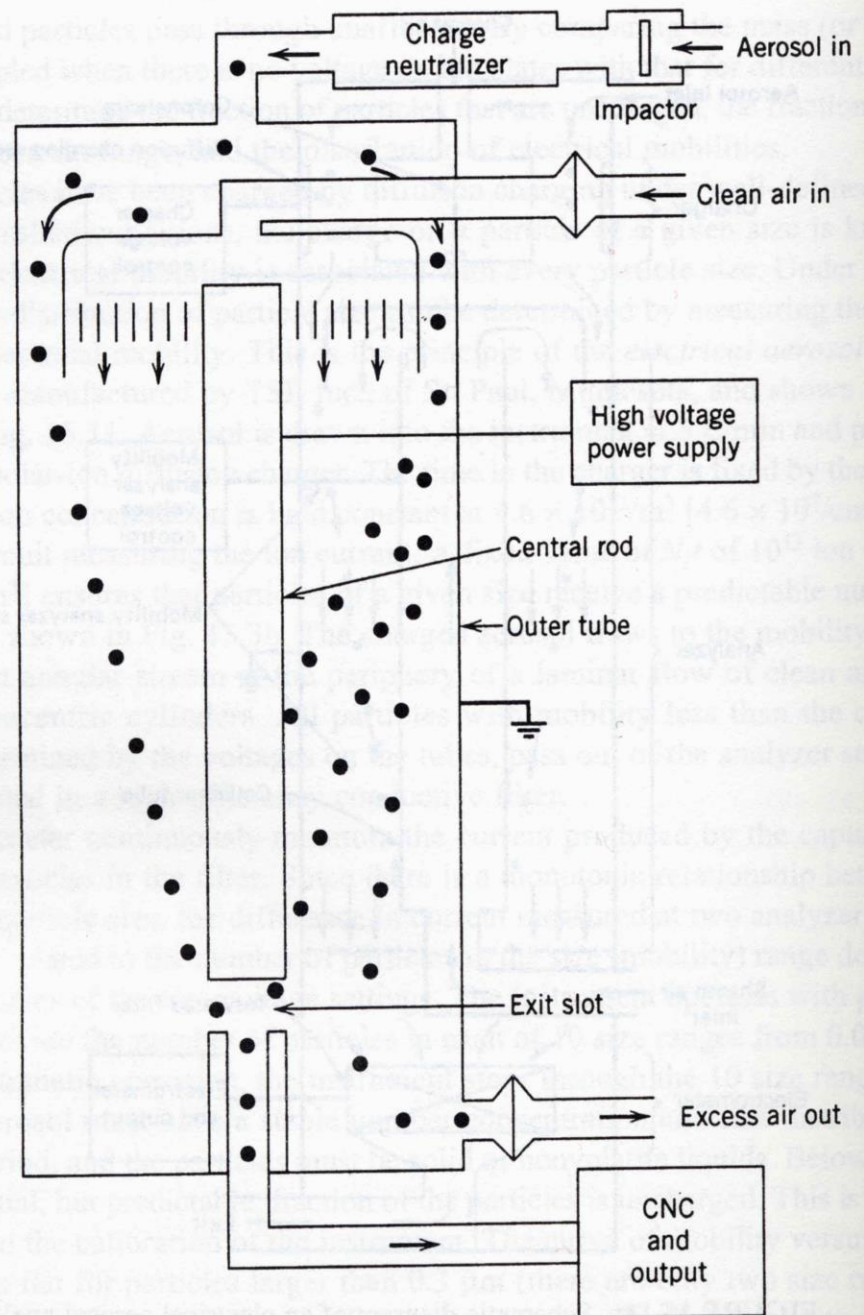


FIGURE 15.12 Schematic diagram of a differential mobility analyzer.



Introduction of **Aerosol Routes** to Electronic and Optical Nanodevice Fabrication

- Clean dry process
- Surfactant/solvent -free process
- Generation of size controllable (uniform) nanoparticles
- Room-temperature deposition minimizing the damage to organic materials
- Exact (nanoscale) positioning of nanoparticles
- Fabrication of well-ordered(patterned) nanostructures (multiscale, multi-dimensional)
- Possibility in scaling-up, not a batch but a continuous process



Seoul National University

*Global Frontier Center
for Multiscale Energy Systems*

Mostly wet processes were used.

Wet Processes

- **Contamination problem due to the existence of solvent and surfactants**
- **Difficulty in exact(nanoscale) positioning of nanoparticles**
- **Inherent batch process**
- **Difficulty in generating well-ordered nanostructures**



Seoul National University

*Global Frontier Center
for Multiscale Energy Systems*

Our Method : Ion Assisted Aerosol Lithography(IAAL) :
Electric-field Assisted Aerosol Lithography (EAAL)
(Nature Nanotechnology(2006), Nano Letters(2011))

- **Charged aerosol nanoparticles** are precisely positioned on the desired location **via focusing electrostatic field**.
- This is a parallel **atmospheric process** with nanoscale resolution on large surface area.



Aerosol positioning and assembling of nanoparticles

- As particle size decreases, thermal driven random Brownian motion of nanoparticles becomes significant.

$$\sqrt{\langle x^2 \rangle} = \sqrt{\frac{2k_B T t}{f}} = \sqrt{2Dt}$$

k_B : Boltzmann _ constant, T : Temperature,

f : friction _ coefficient

t : time, D : Diffusion _ coefficient of particle



Seoul National University

Global Frontier Center
for Multiscale Energy Systems

Aerosol Positioning and assembling of nanoparticles

Particle size	D (cm ² /sec)	Brownian random movement at 20°C in 1 second
1μm	2.77×10^{-7}	7μm
100nm	6.75×10^{-6}	37μm
10nm	5.24×10^{-4}	320μm
1nm	5.14×10^{-2}	3200μm (= 3.2mm)

- Precise positioning of nanoparticles is required for nanoscale assembly of nanoparticles.

➔ Suppression of thermal motion of nanoparticles is necessary.

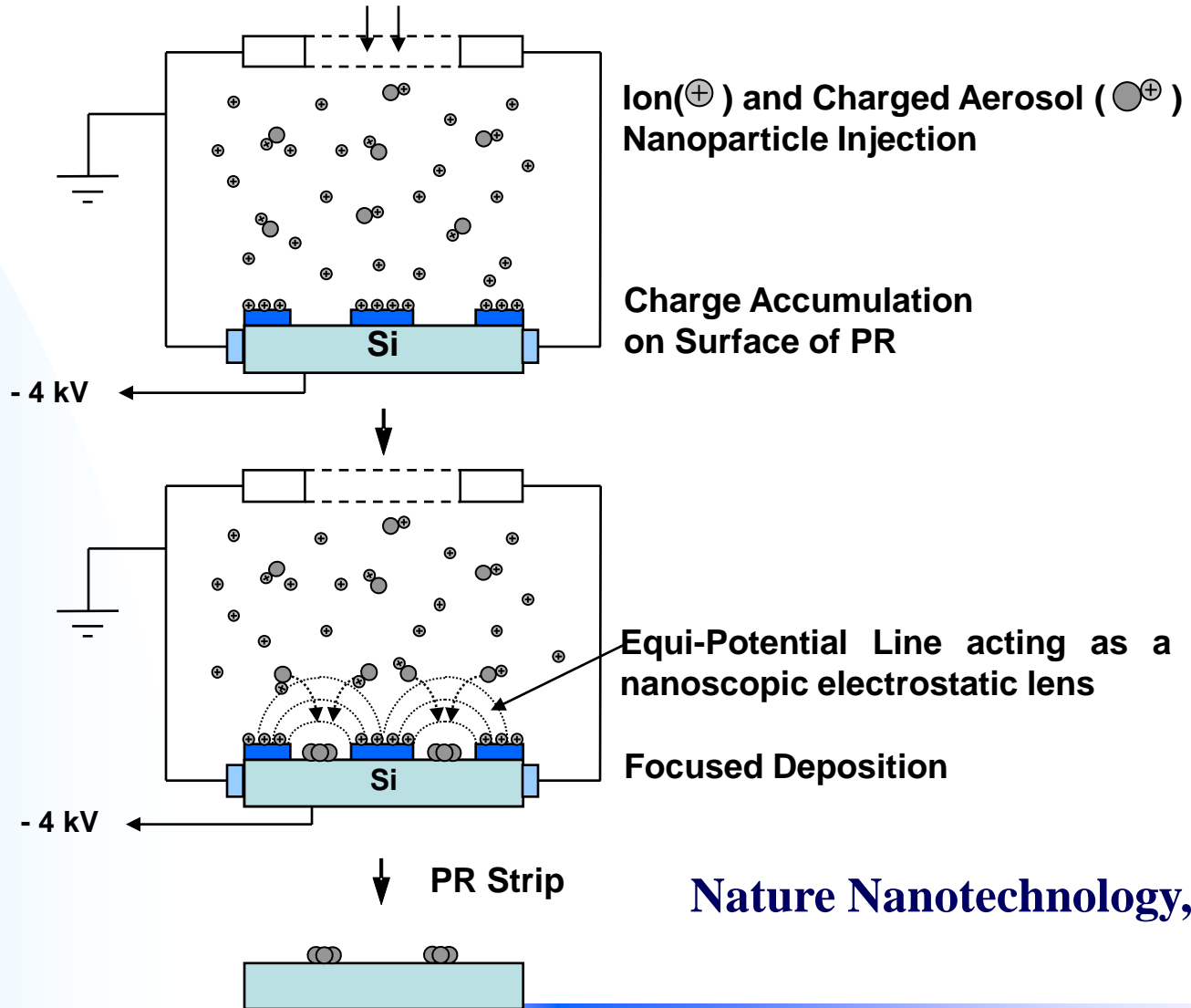
➔ Electrostatic force is utilized to suppress random Brownian particle deposition .



Seoul National University

*Global Frontier Center
for Multiscale Energy Systems*

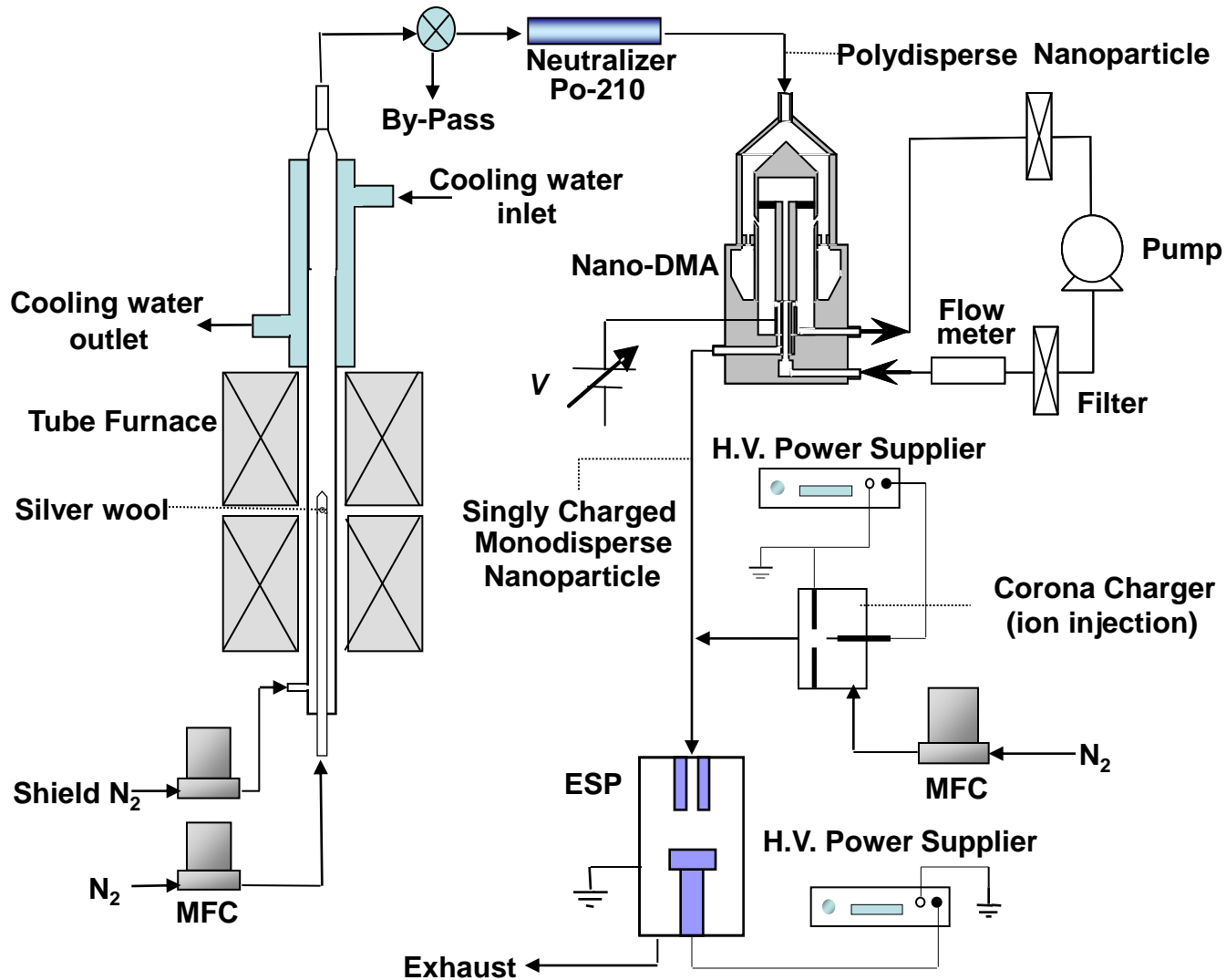
Ion Assisted Aerosol Lithography



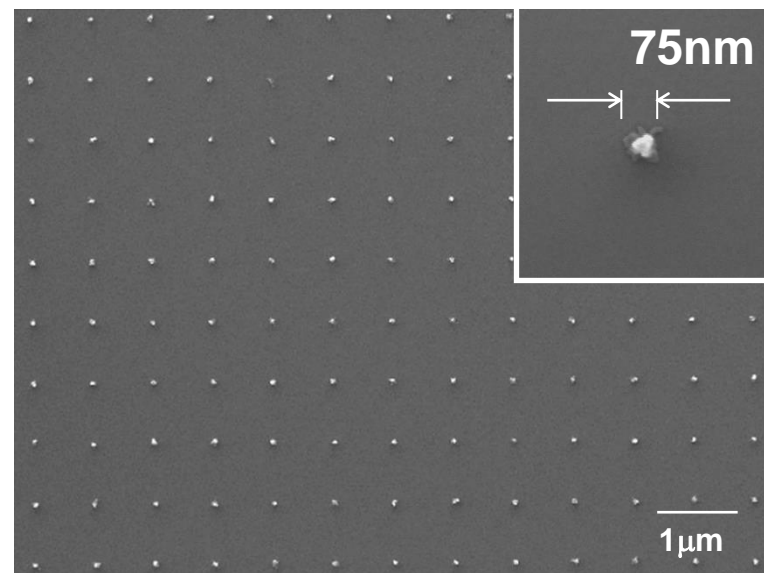
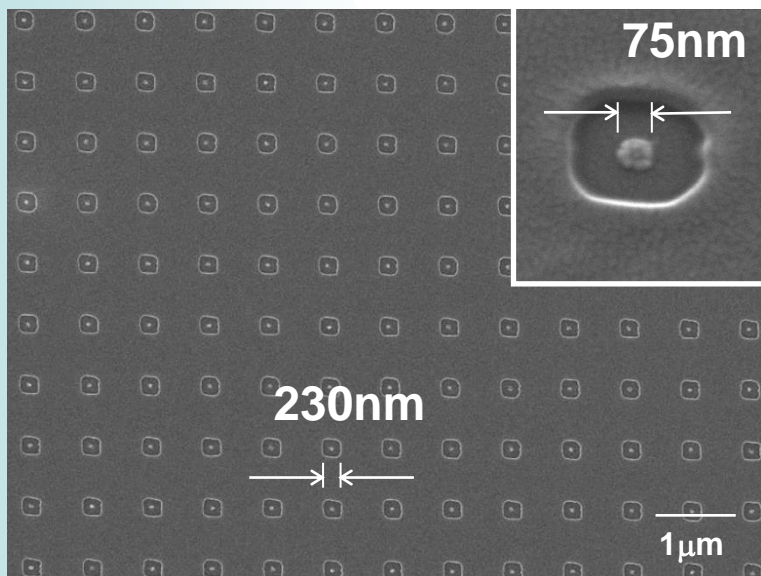
Nature Nanotechnology, 2006



Experimental setup

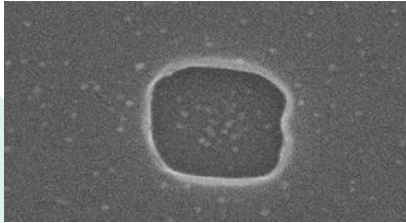


With ion injection: PR layers act as a means to generate nanoscopic electrostatic lenses

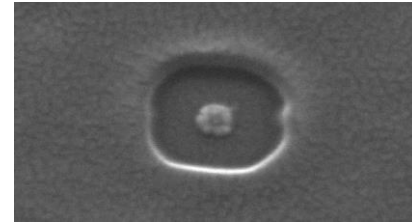


Nanoscale electrostatic lenses

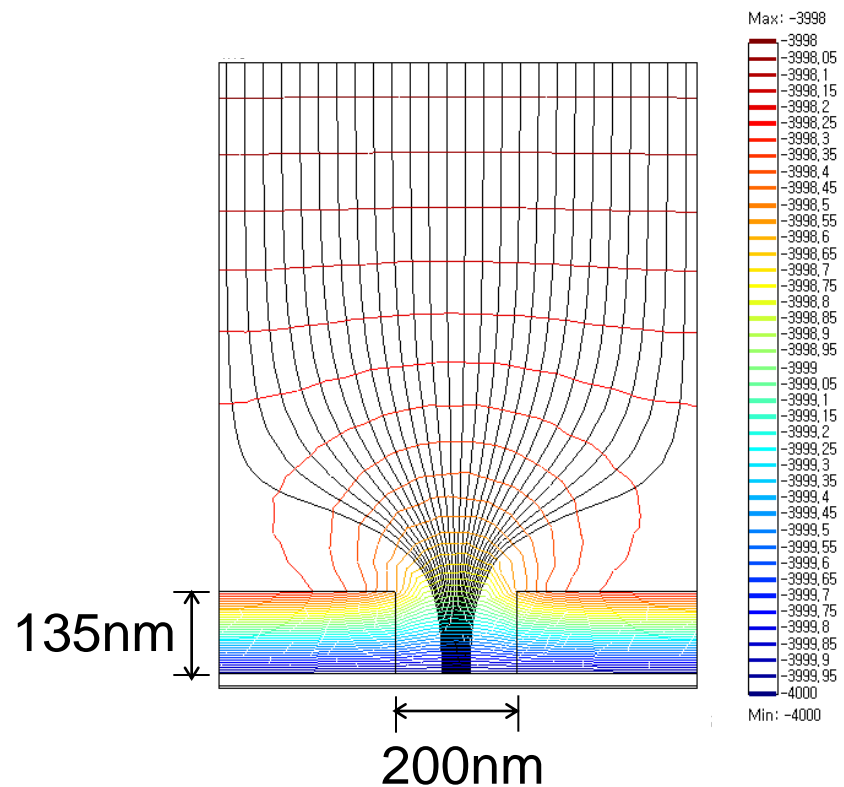
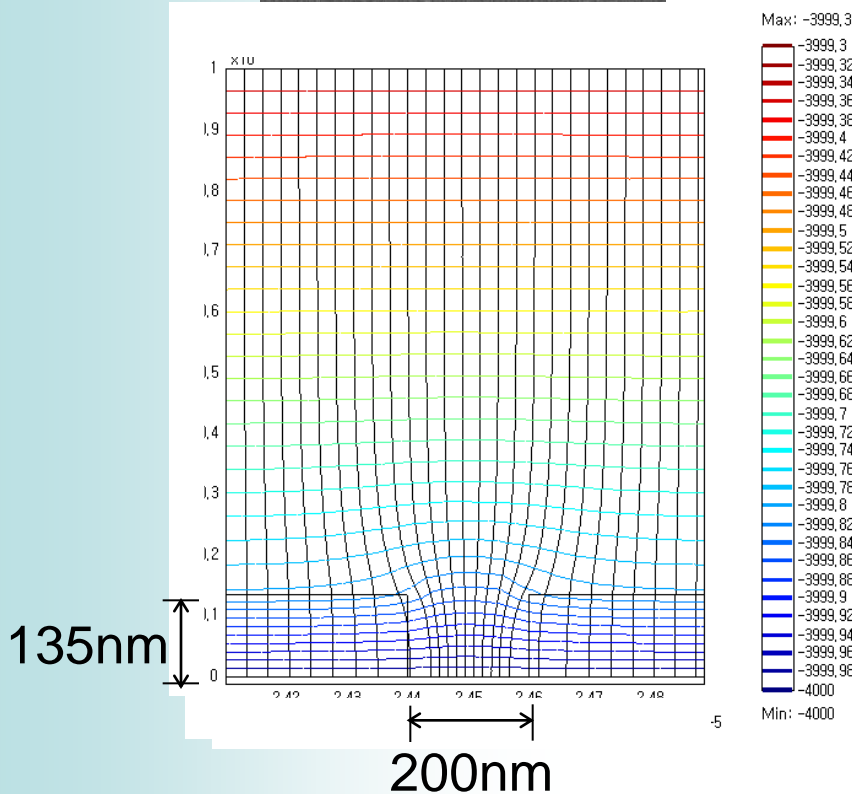
▶ without ion injection



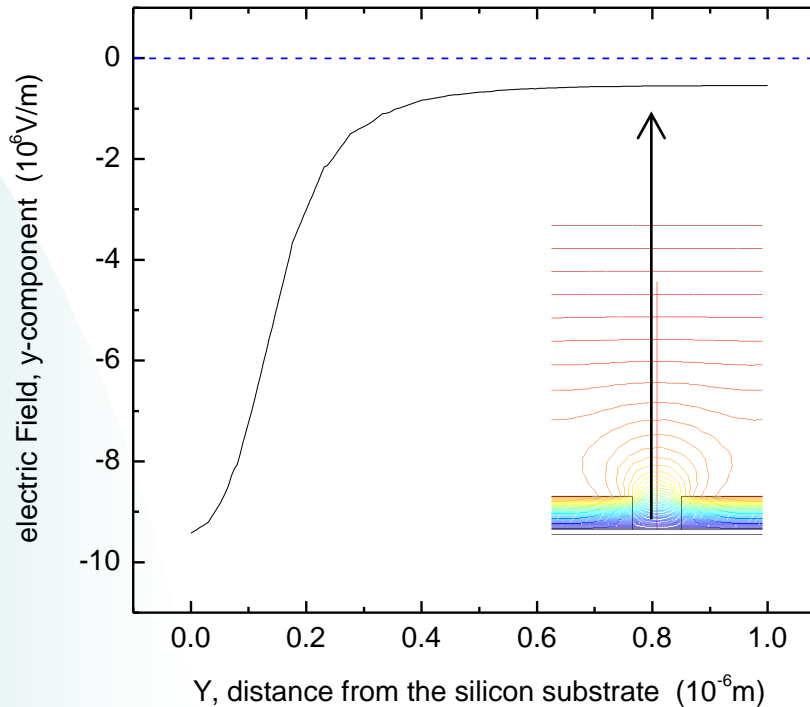
▶ w/ ion injection (41pm)



**Ion mobility
vs particle
mobility**



Suppression of thermal motion of particles near surface by using electrostatic focusing lens.



The field strength near the lens region would reach $3 \times 10^6 \text{ V/m}$. The kinetic energy due to this electric field induced particle velocity would be about **600 meV** which is much higher than random thermal energy of particles ($\sim k_B T = 30 \text{ meV}$).

Kinetic energy due to electric field induced particle velocity
 $\sim 600 \text{ meV}$

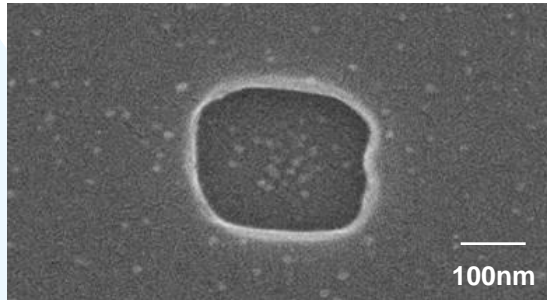
\gg Random thermal energy $\sim 30 \text{ meV}$



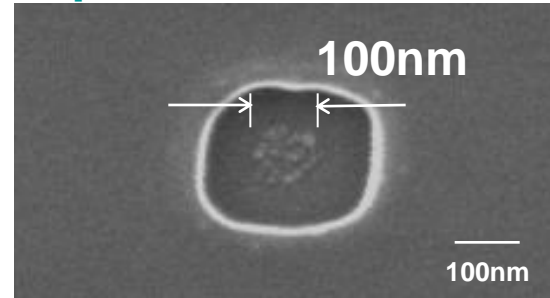
Focusing effect with the increase of ion flow rates

(Nature Nanotechnology, 1, 117, 2006)

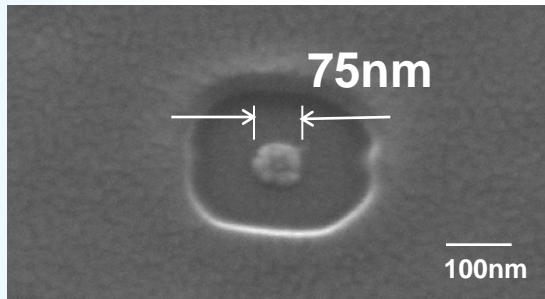
0lpm



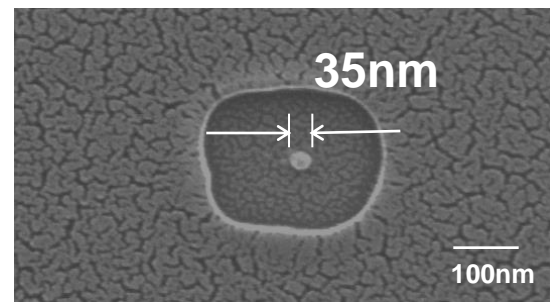
3lpm



4lpm



6lpm



Simulation of Electrodynamic Focusing of Charged Aerosols

● Particle Trajectories : Langevin Equation

$$m_p \frac{d\vec{v}_p}{dt} = \vec{F}_D + \vec{F}_B + \vec{F}_E + \vec{F}_W$$

\vec{F}_D : Fluid Drag Force

\vec{F}_B : Brownian random Force

\vec{F}_E : Electric Force

\vec{F}_W : Van der Waals Force

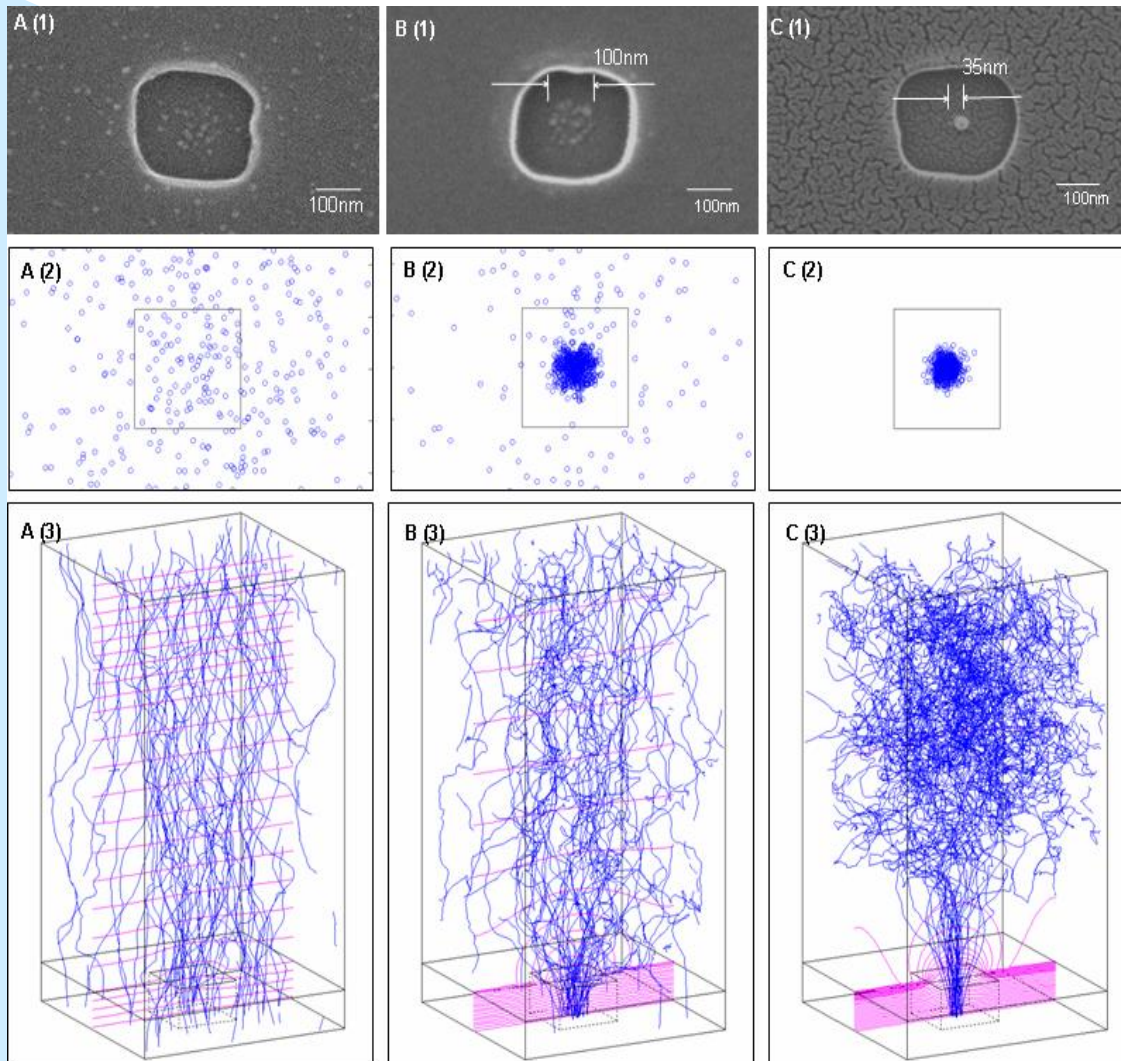
● Electric Field : COMSOL CODE



Seoul National University

*Global Frontier Center
for Multiscale Energy Systems*

Simulation Results (Journal of Aerosol Science, Nov., 2007)



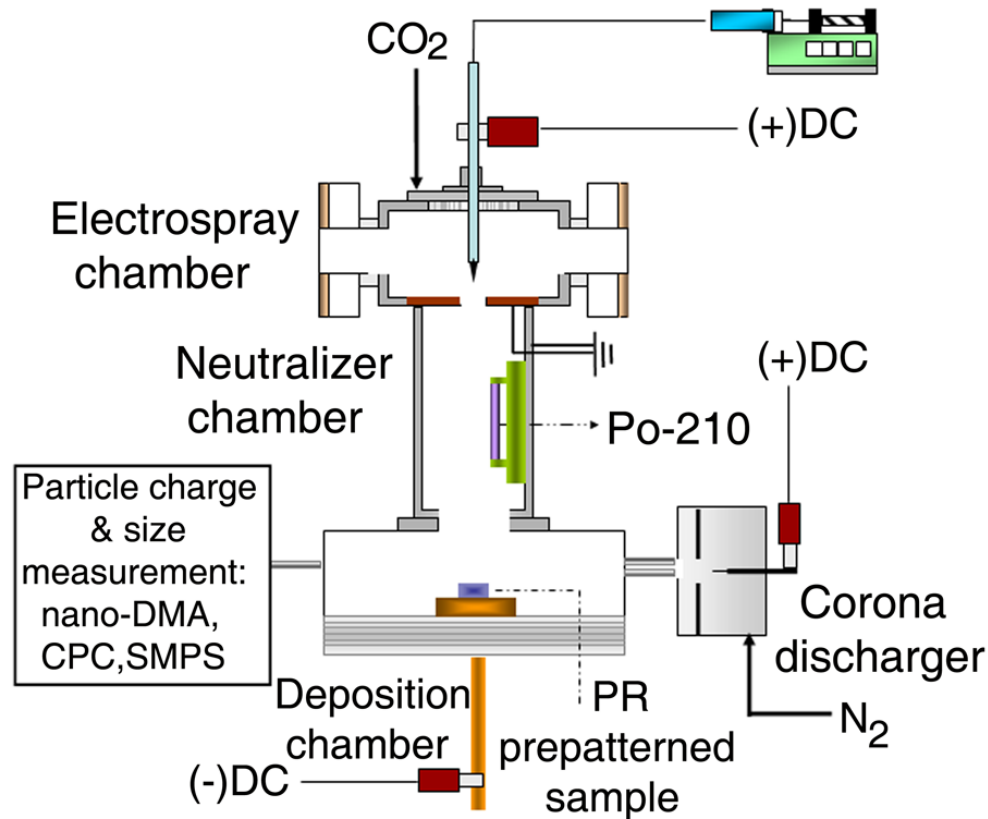
- A. No ion injection**
- B. With ion injection, N₂ 3lpm**
- C. With ion injection, N₂ 6lpm**



Patterning of nanoparticles that were already made

Electrospray of nanoparticle suspension

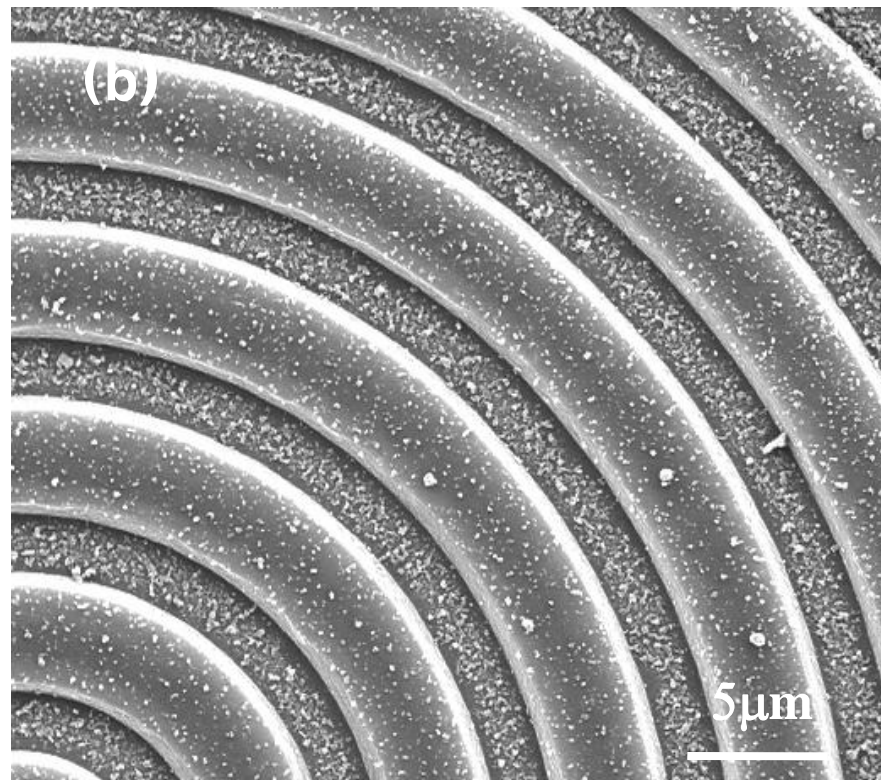
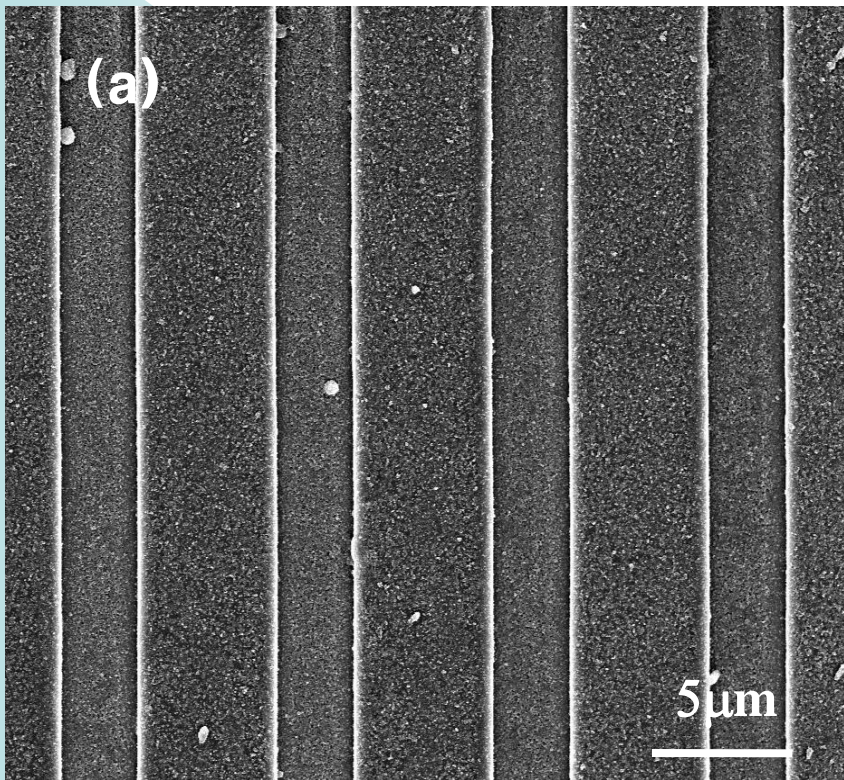
(Applied Physics Letters, 94, 053104, 2009)



Seoul National University

Global Frontier Center
for Multiscale Energy Systems

30nm Polystyrene nanoparticles



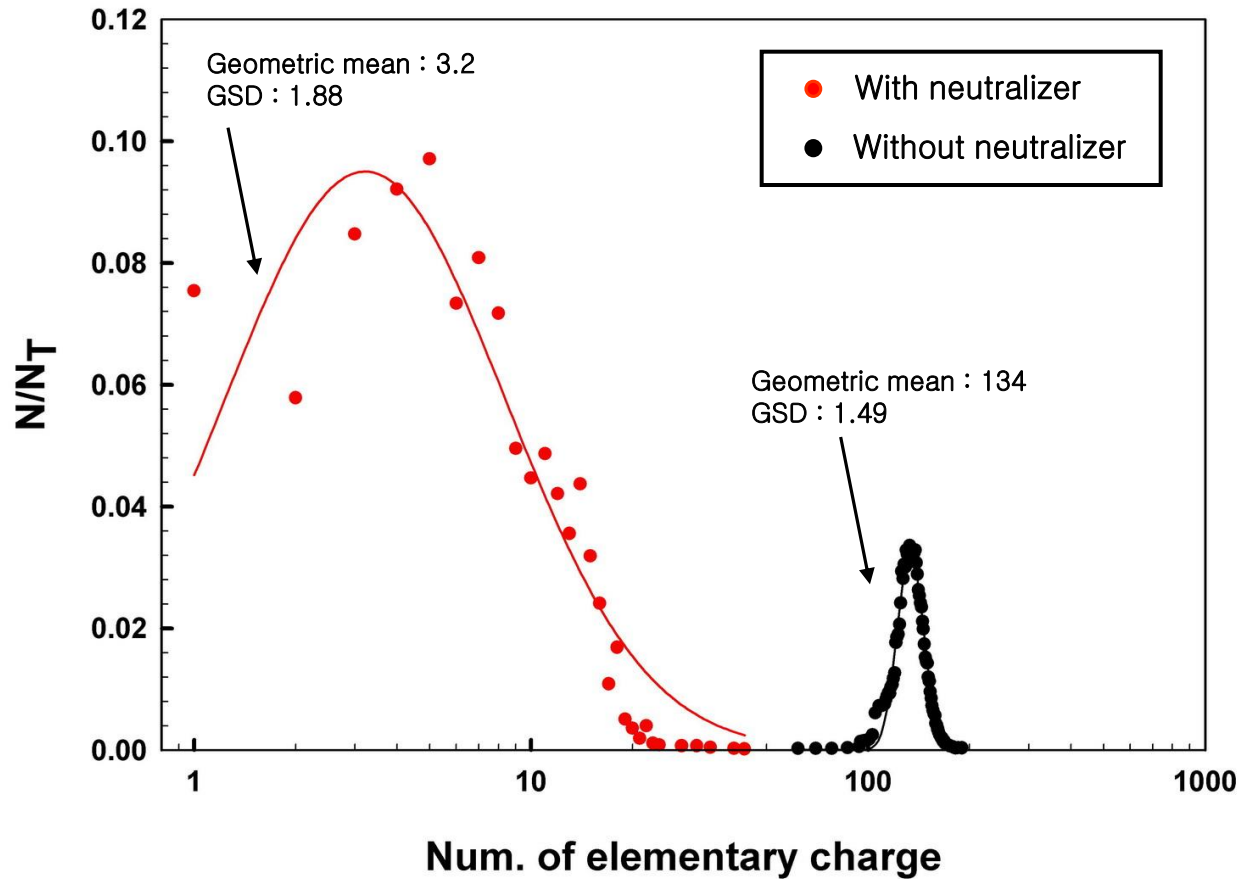
Ion shower 30min,
Deposition 30min,
Without neutralizer

$V_s = -$
4kV



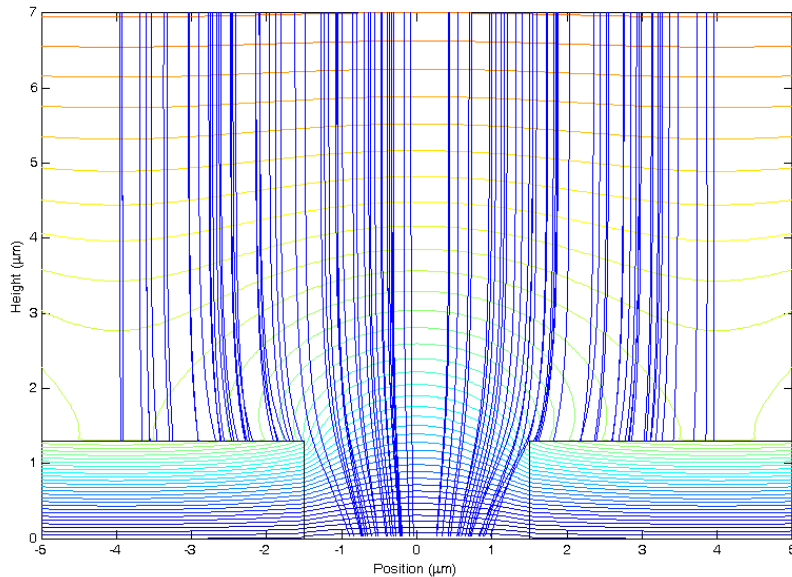
Seoul National University
Global Frontier Center
for Multiscale Energy Systems

Results – Charge Distribution

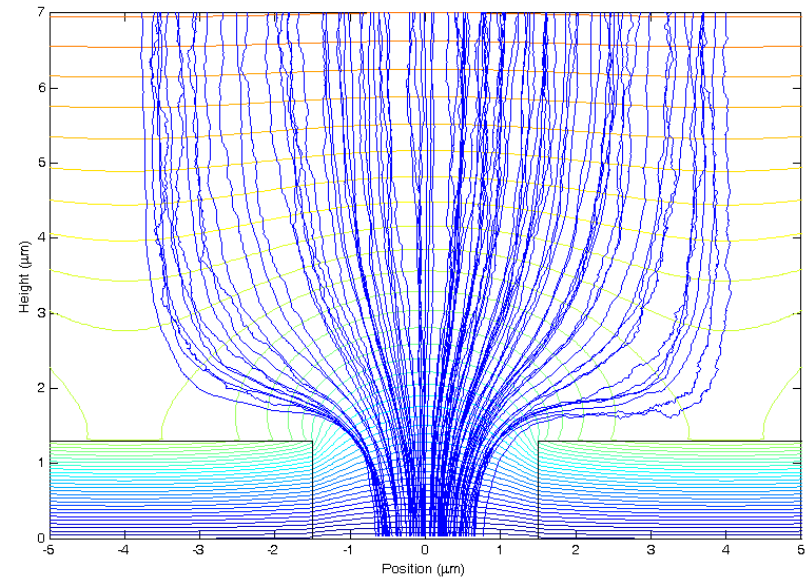


Inertial effect of 10 nm particles: Too high charge, too high velocity

(a)



(b)



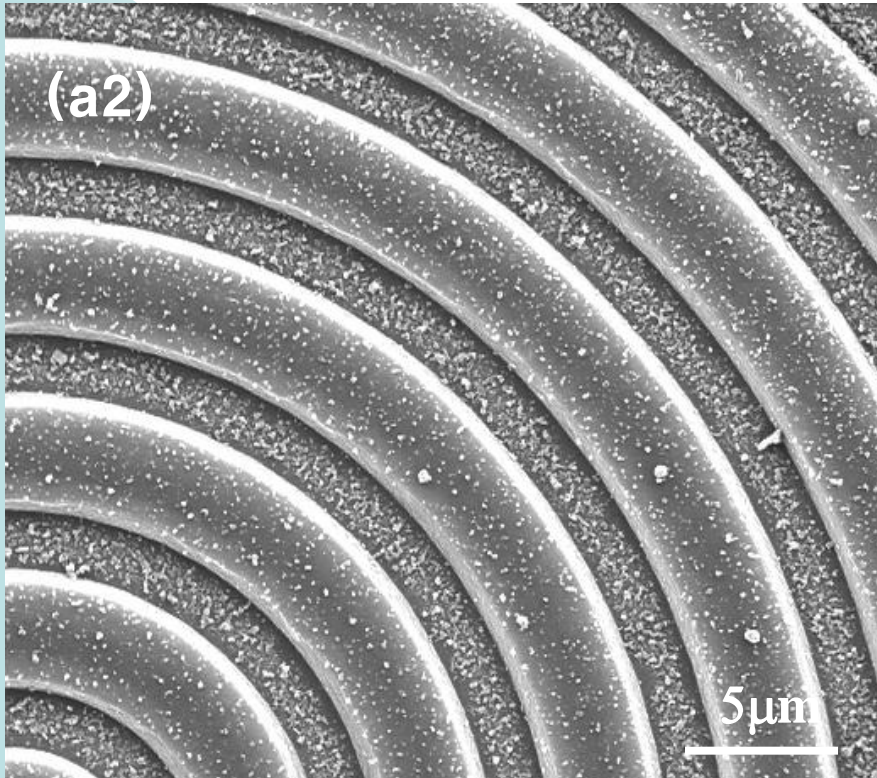
Ion shower 30min,
Deposition 30min,
W/O neutralizer
 $V_s = -4\text{kV}$

<3μm line pattern>

Ion shower 30min,
Deposition 30min,
W/ neutralizer
 $V_s = -4\text{kV}$

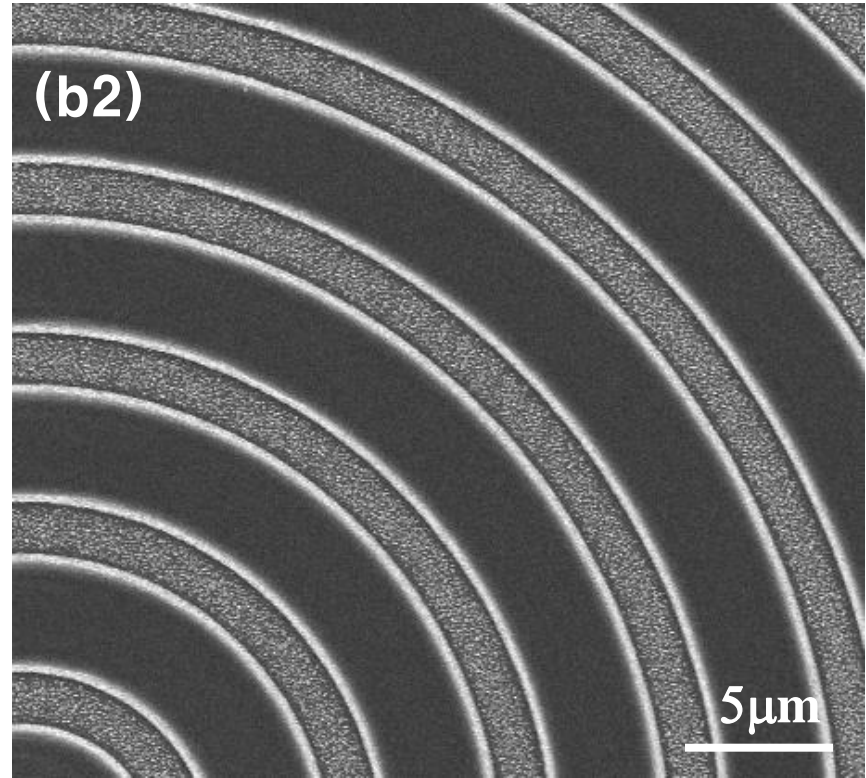


Results – Effects of neutralizer 2



Ion shower 30min,
Deposition 30min,
W/O neutralizer
 $V_s = -4\text{kV}$

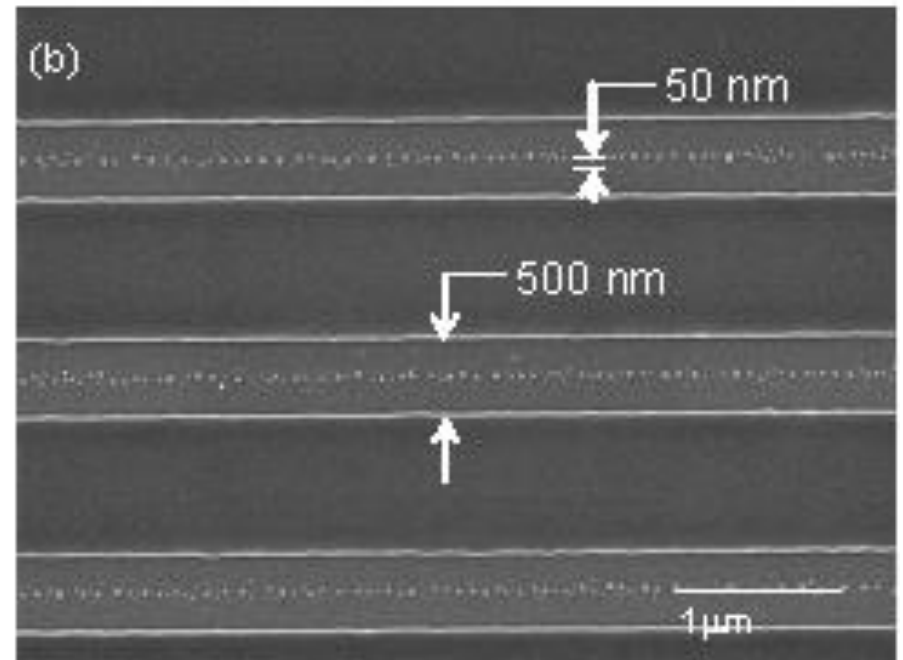
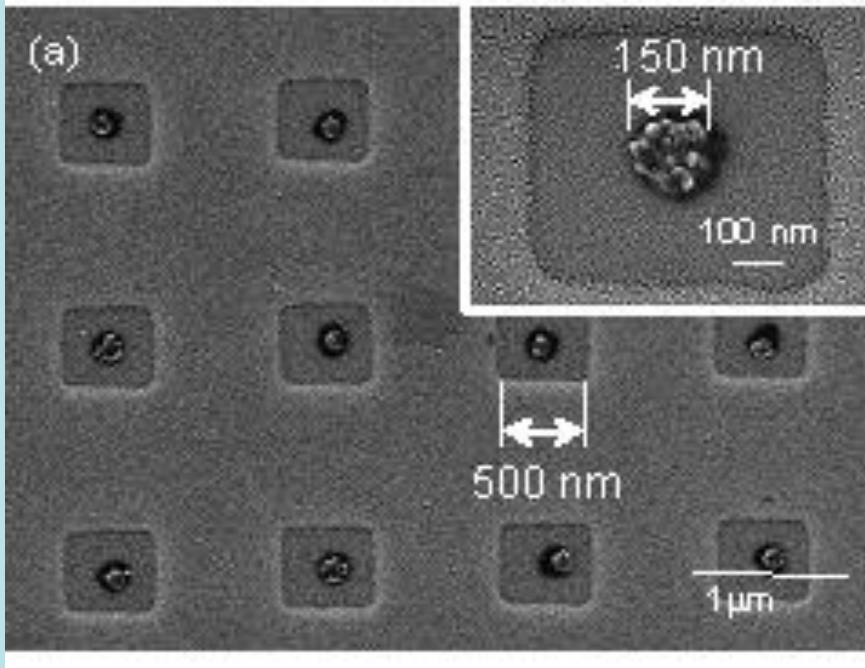
<2μm circle pattern>



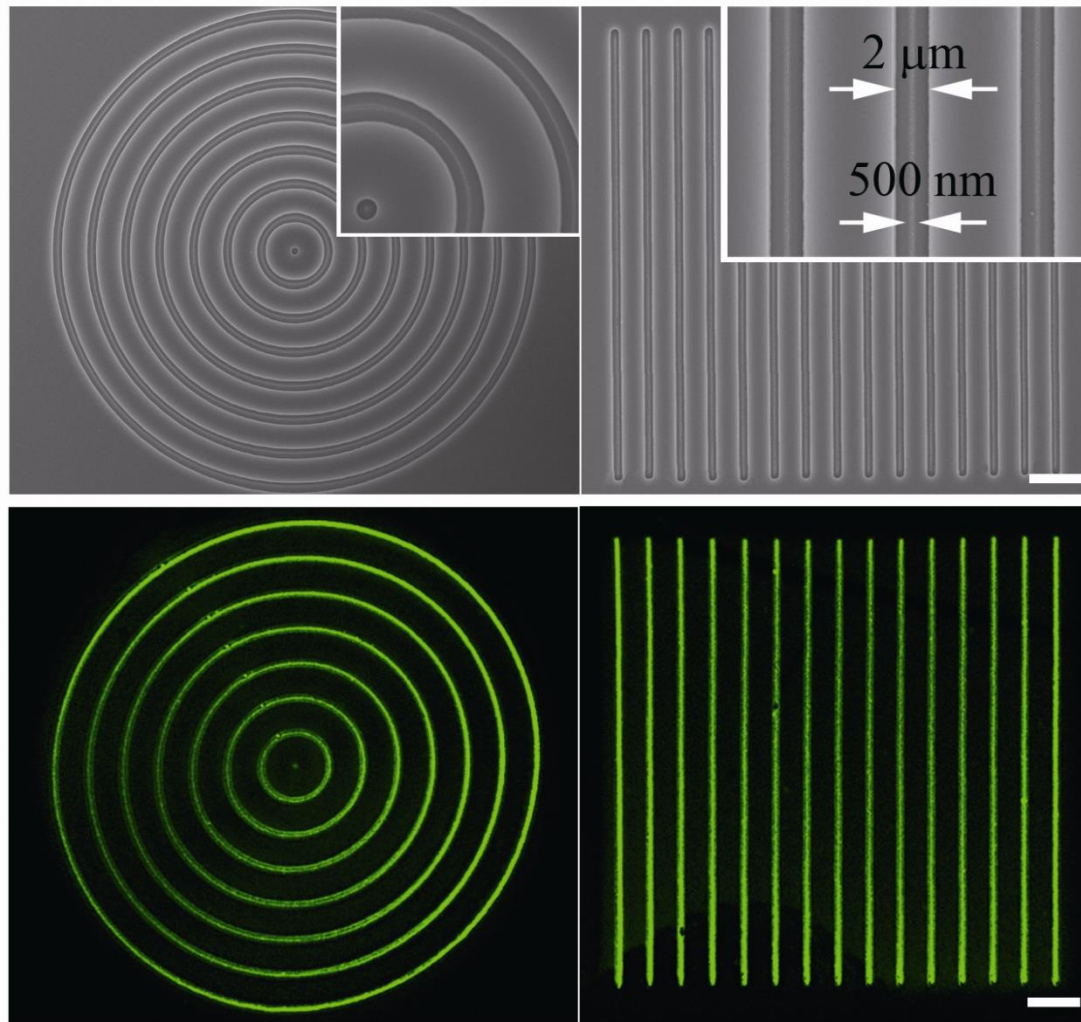
Ion shower 30min,
Deposition 30min,
W/ neutralizer
 $V_s = -4\text{kV}$



Focused patterning of 20nm gold nanoparticles



Protein Patterning(Human IgG)(Small, 7, 1790, (2011))

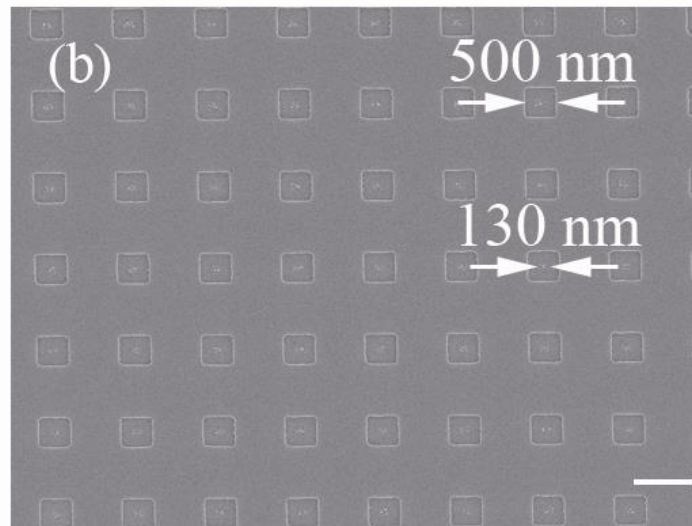
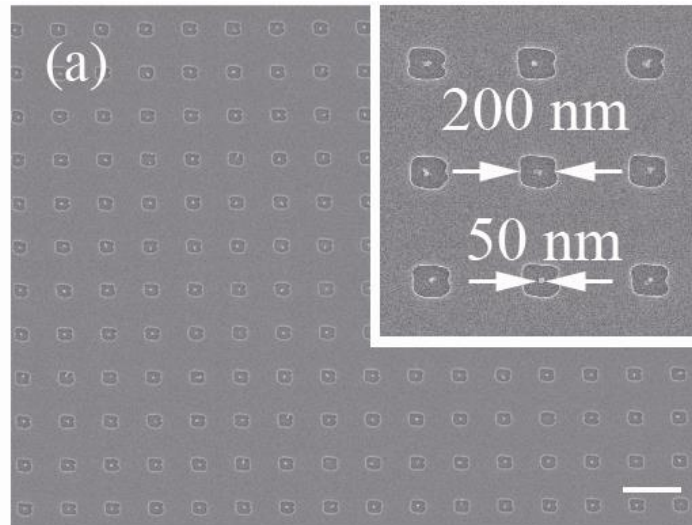


<scale bar = 10 μm >



Protein Patterning – nanoscale, parallel method

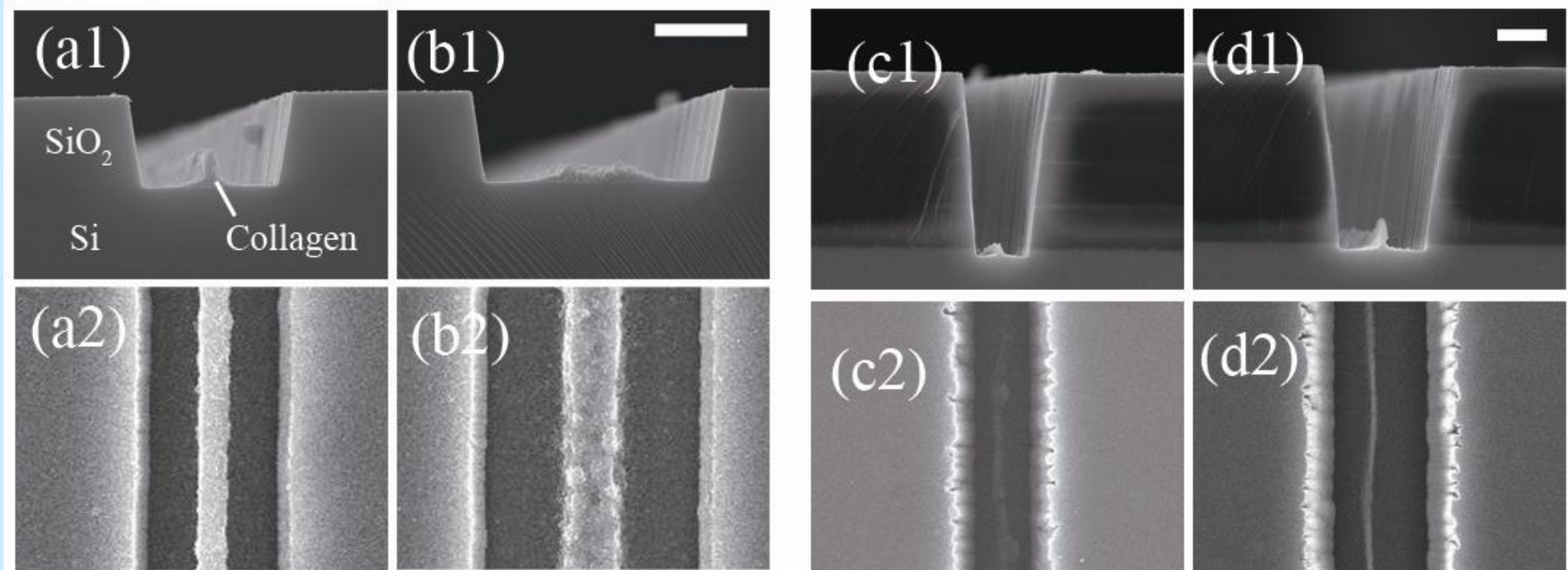
(Small, 2011)



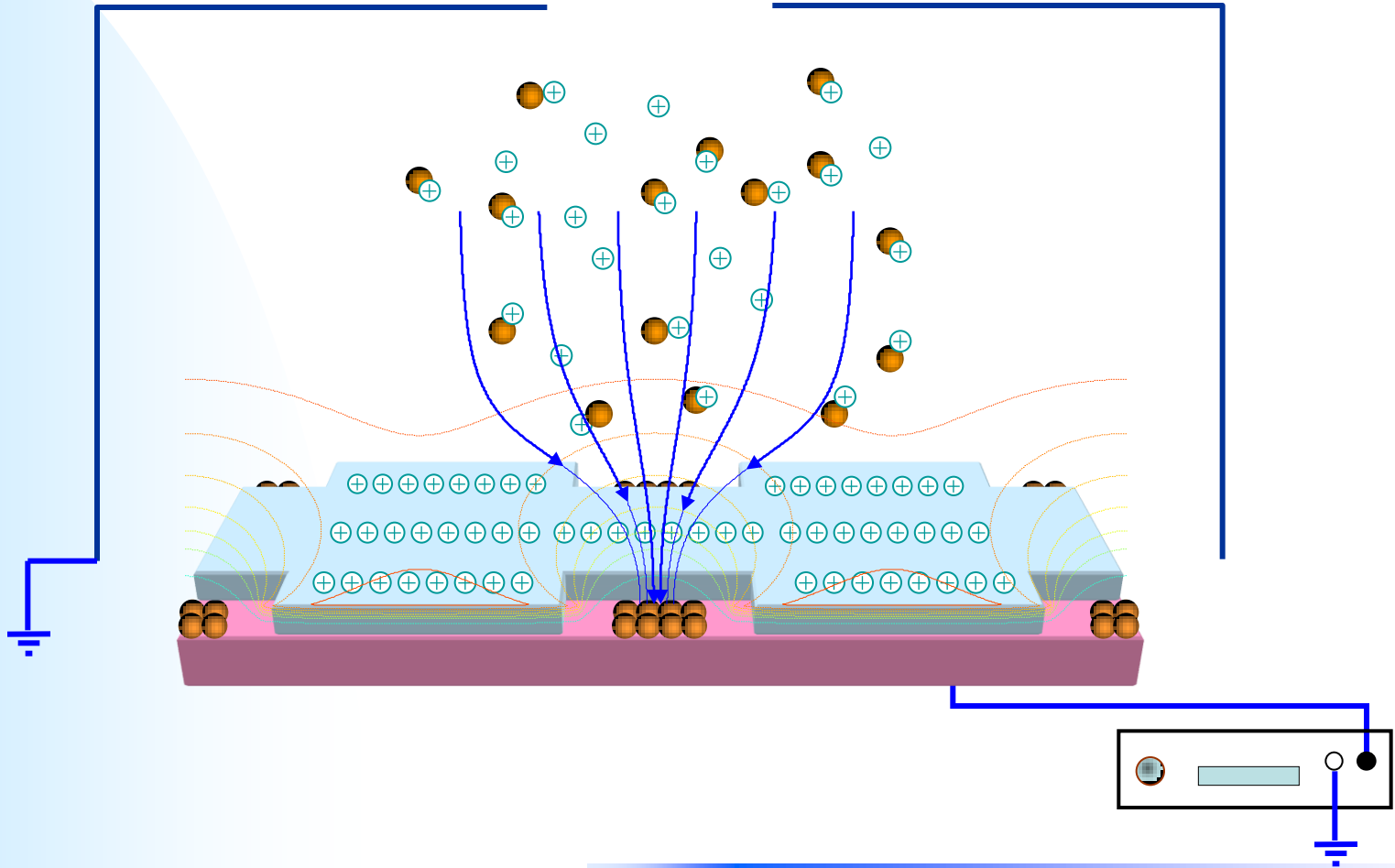
<scale bar = 1 μ m>



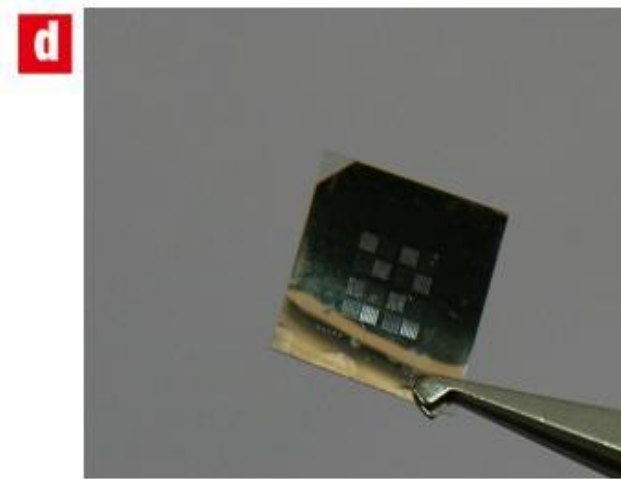
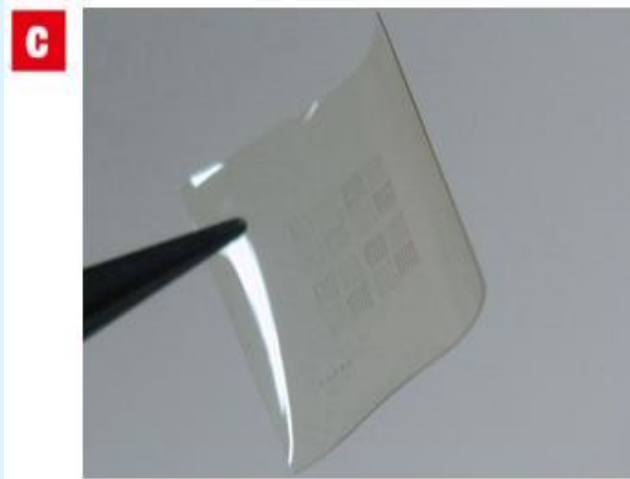
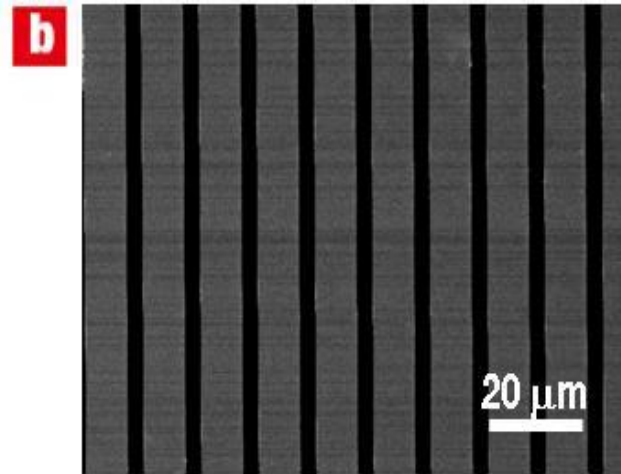
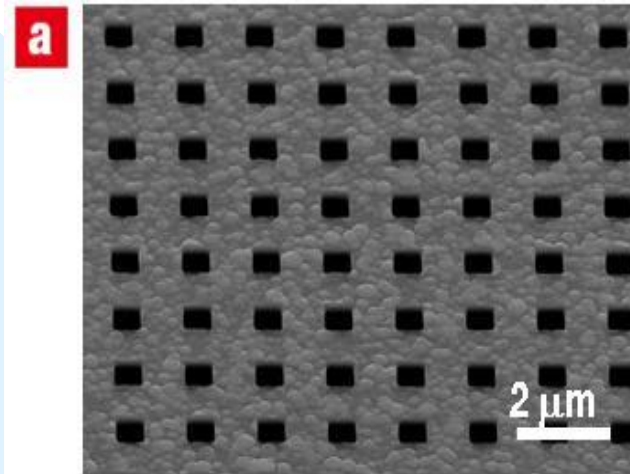
Protein Patterning in microfluidic channels



Do we need resist prepatterning ? Can we eliminate photo resist patterning step ? **Solution : Nanoparticle Focusing Mask** (*Small*, Vol. 6, p 2146, 2010)

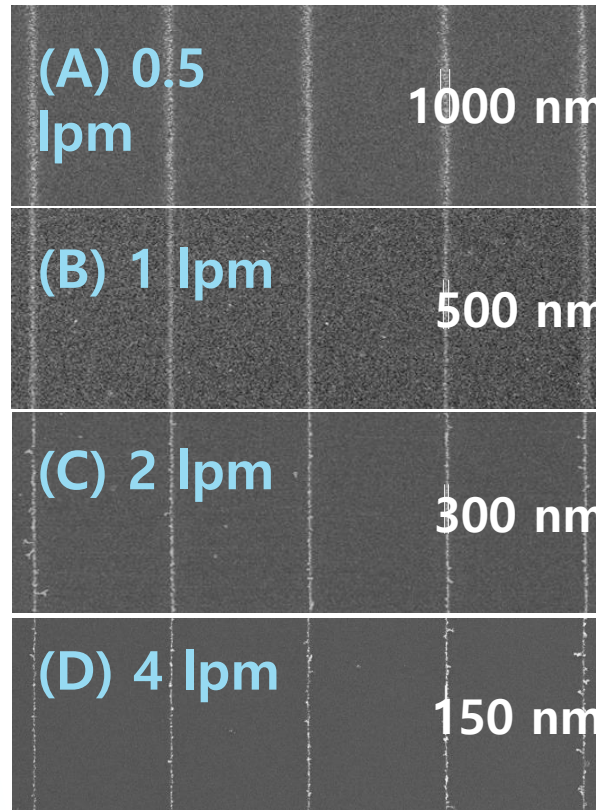


Nanoparticle Focusing Mask

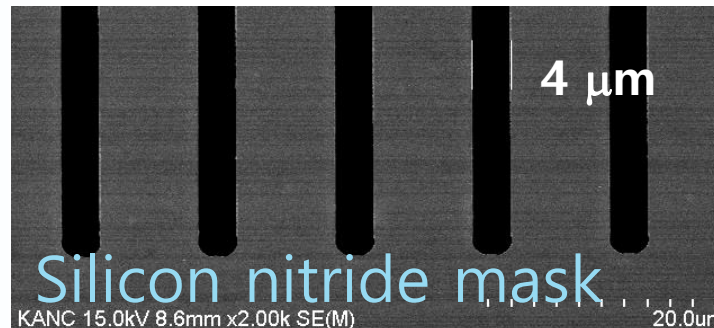


Size Control by Ion Flow Rate

(Small, Vol. 6, p 2146, 2010)



4 μm \rightarrow 0.15 ~ 1 μm

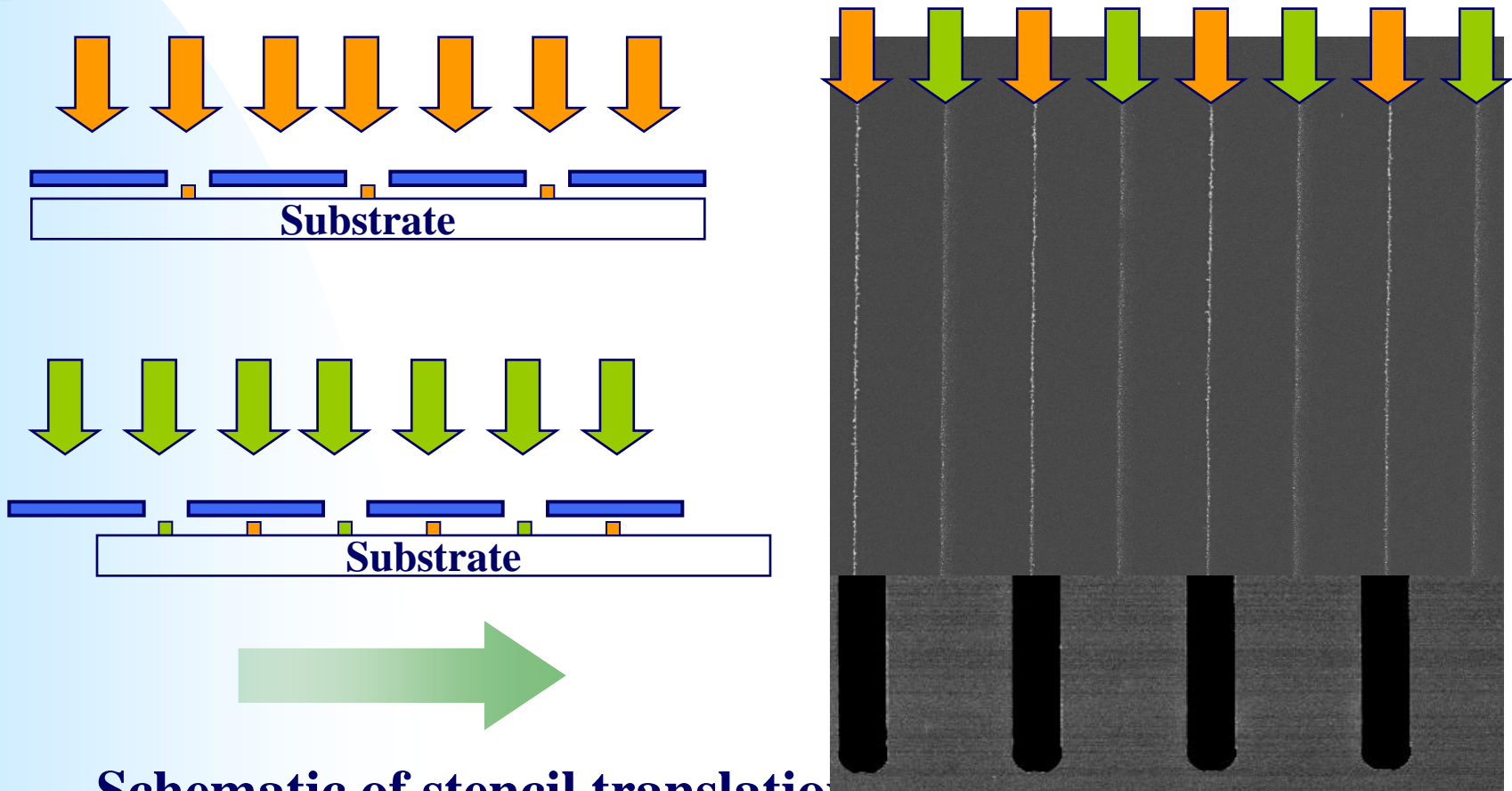


ional University

Global Frontier Center
for Multiscale Energy Systems

Sequential Deposition

➔ Control the space between patterns by sequential deposition

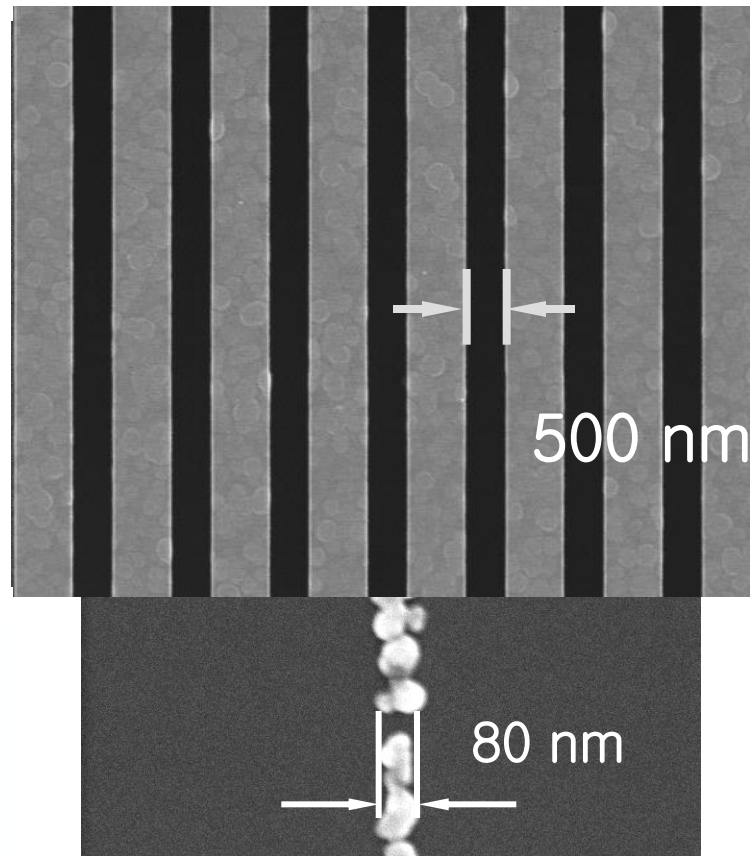


Schematic of stencil translation



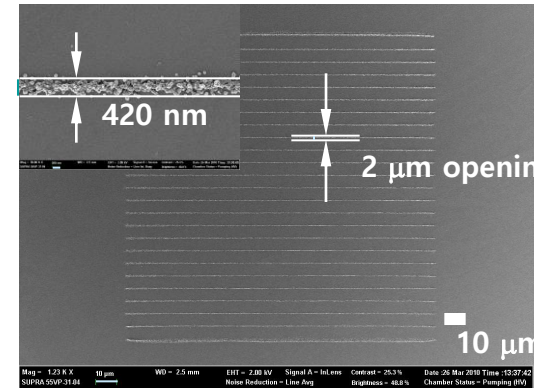
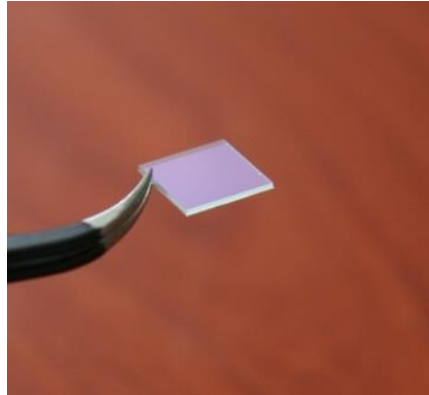
Focusing Nano-Mask

**Focusing Mask with 500 nm line openings
(manufactured by e-beam lithography)**

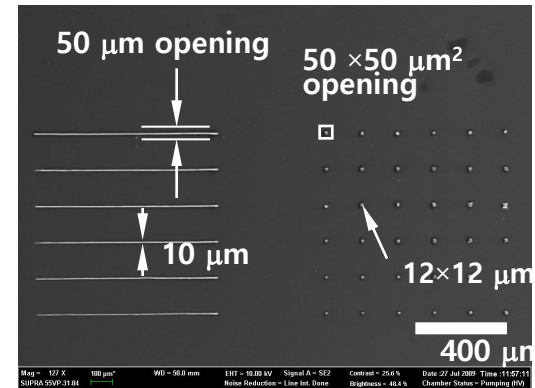
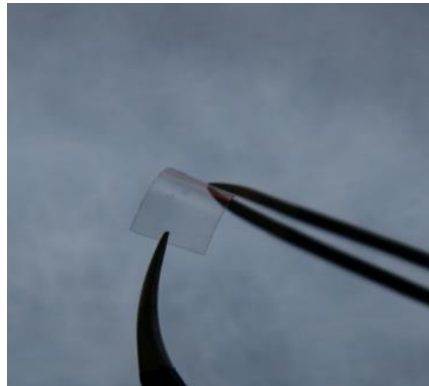


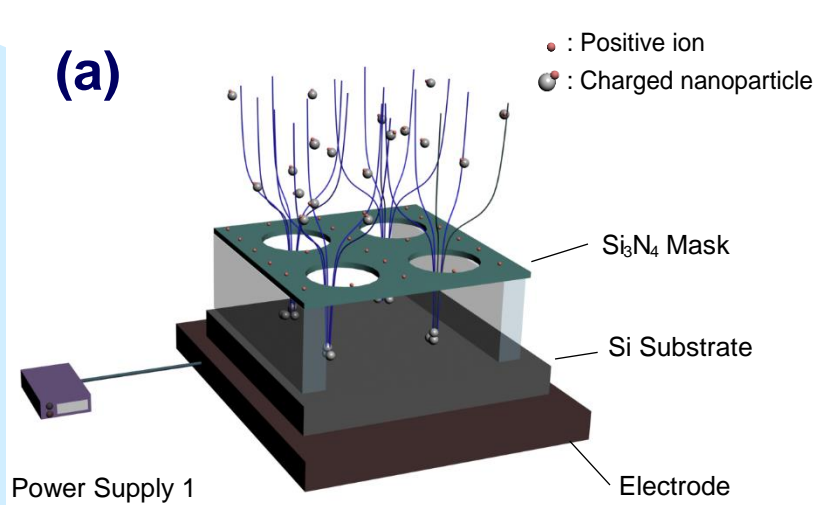
Focused patterning on thick non-conducting substrates (*Small*, Vol. 6, p 2146, 2010)

Patterning of electrospayed 30 nm PSL particles on thick glass (~ 0.7 mm)

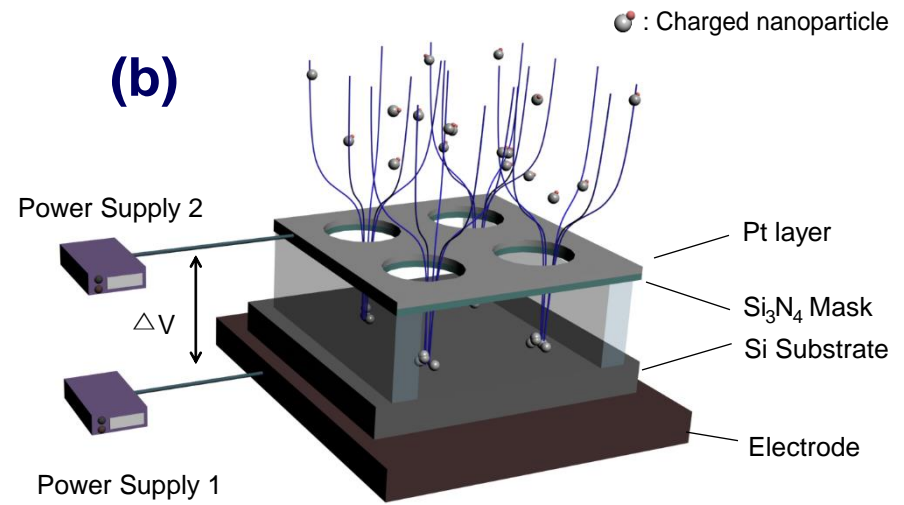


Patterning of electrospayed 100 nm PSL particles on a flexible PET film (thickness ~ 0.1 mm)





IAAL



EAAL

Electrified mask resembles with ion accumulated dielectric mask :

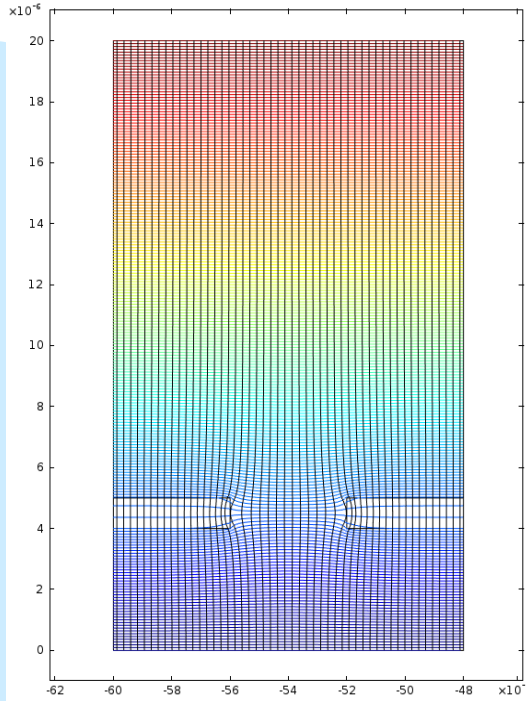
Electric-field Assisted Aerosol Lithography(EAAL)

Journal of Aerosol Science, 2015



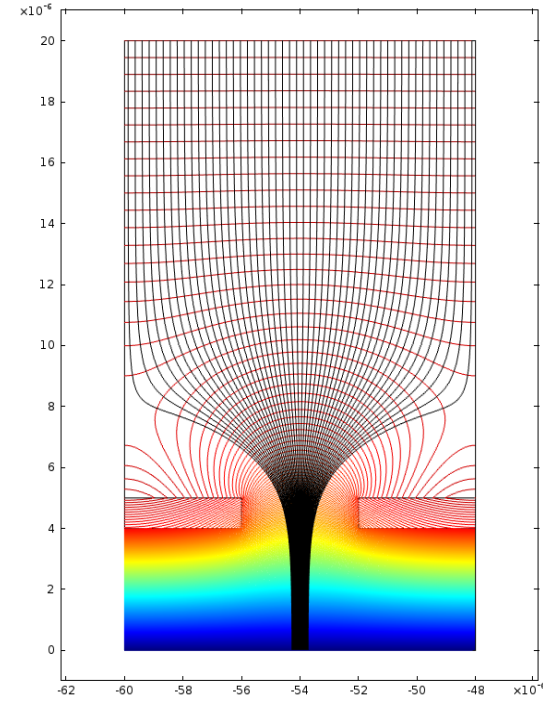
Seoul National University
Global Frontier Center
for Multiscale Energy Systems

(a)



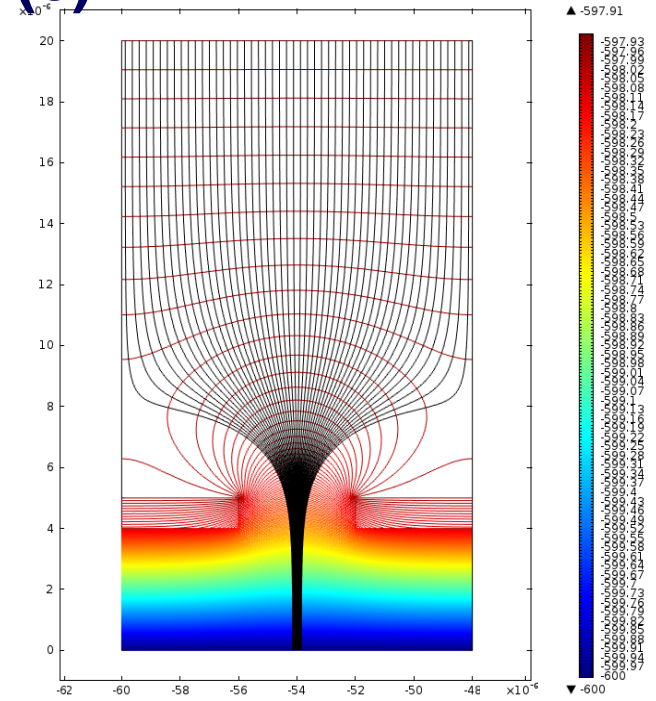
(b)

IAAL



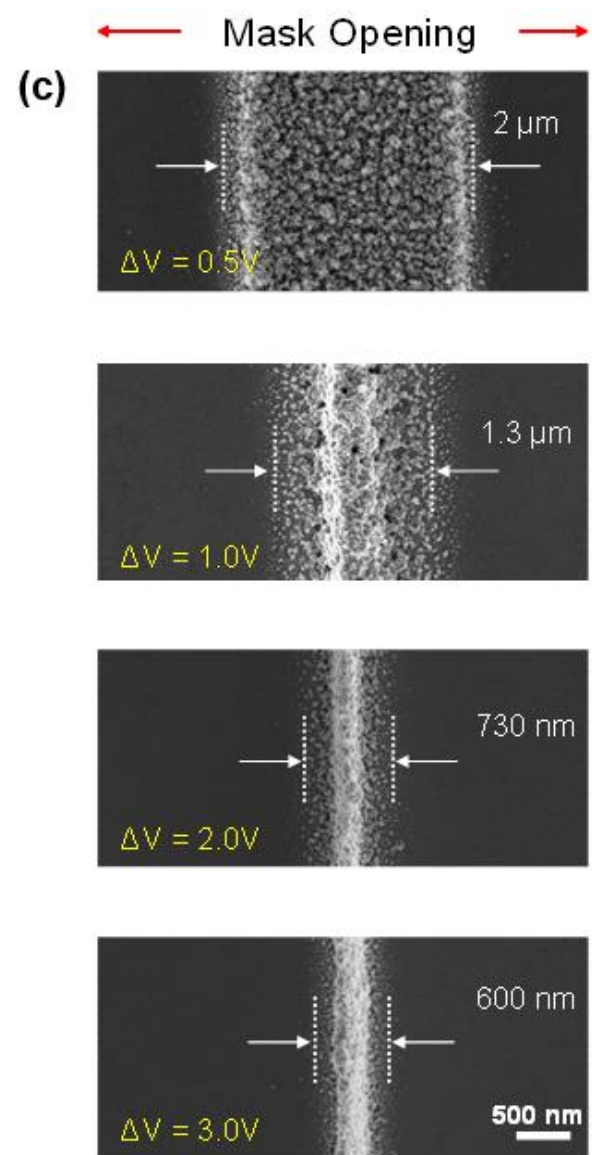
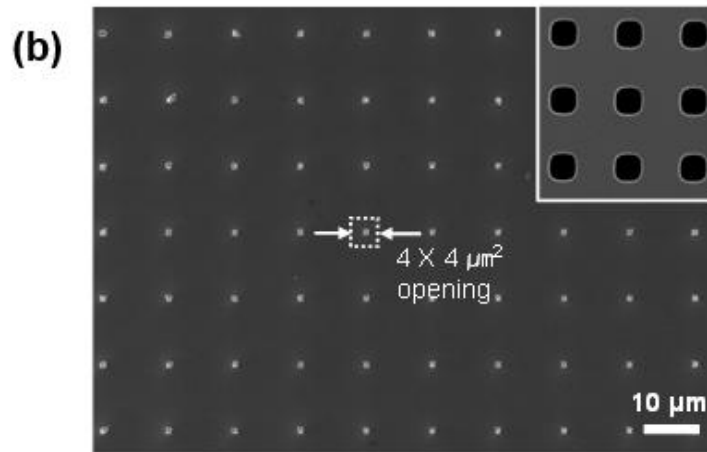
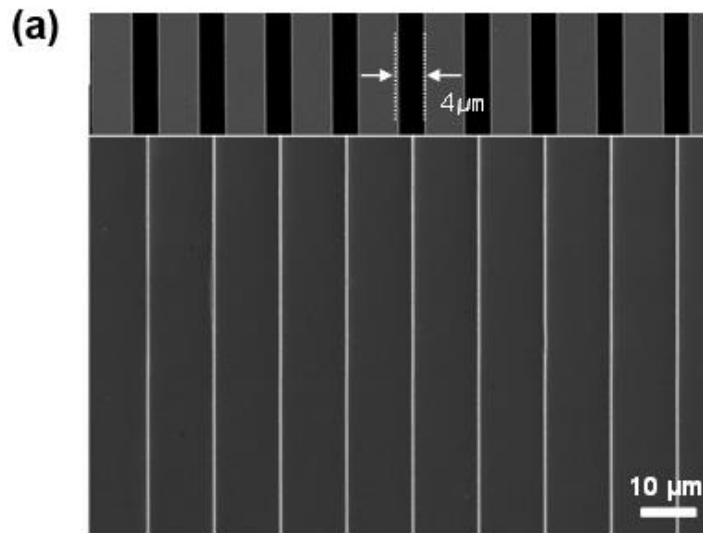
(c)

EAAL



(a) none charge (b) ion accumulated surface charge density ($5.3 \times 10^{-6} \text{ C/m}^2$) (c) electric potential difference between the substrate and the mask layer (2.0 V)

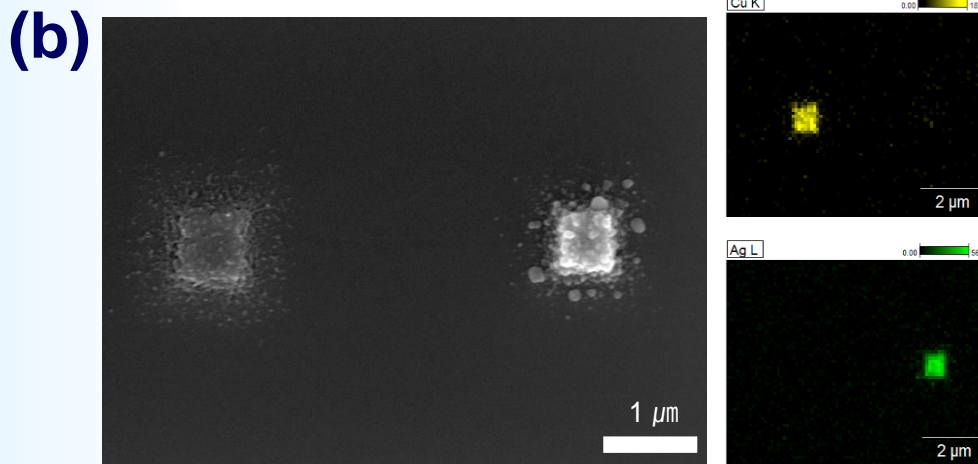
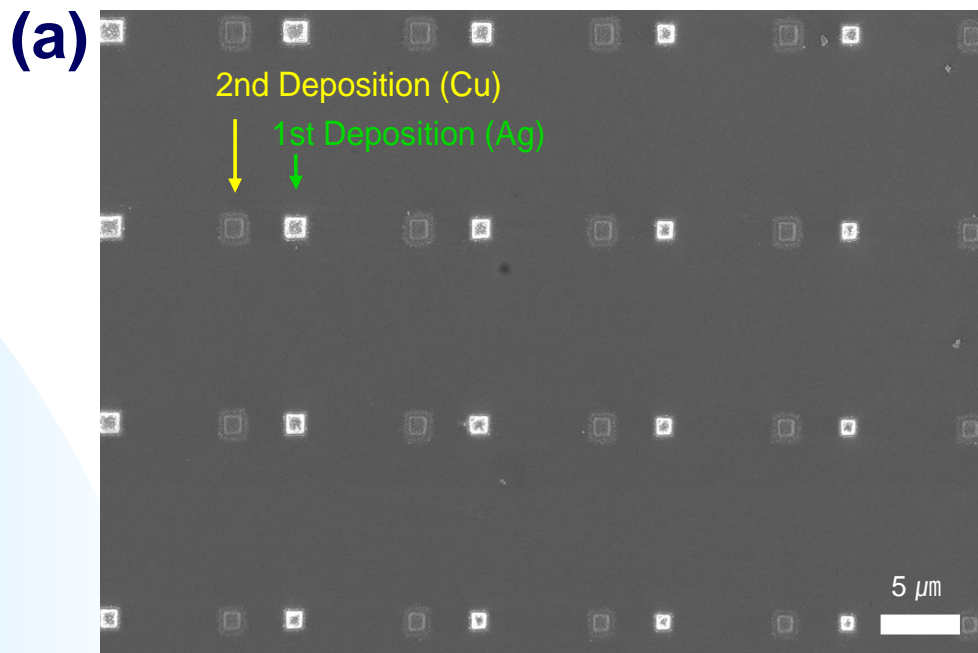




EAAL without ion injection (J. Aerosol Science, 2015)



Seoul National University
 Global Frontier Center
 for Multiscale Energy Systems



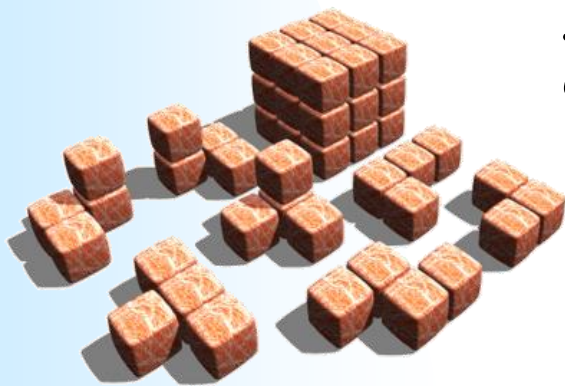
**Journal of Aerosol Science
2015**

Offset multi-material nanoparticle cluster array formation using mask translation.



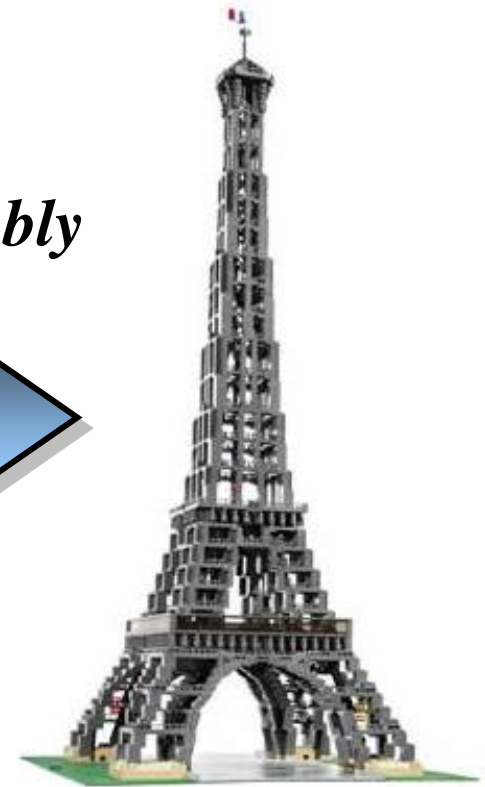
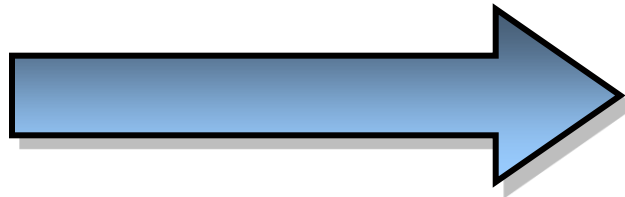
Seoul National University
Global Frontier Center
for Multiscale Energy Systems

The next task is to assemble nanoparticles in three dimensions.



Nanoparticles

*3 Dimensional Assembly
of Nanoparticles ?*



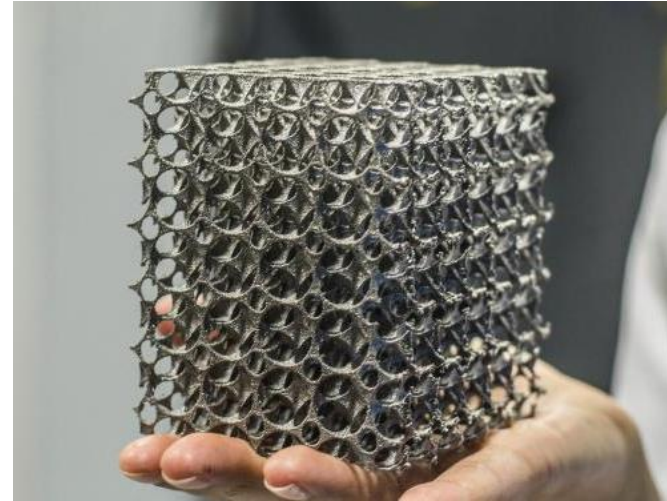
Nanotechnology



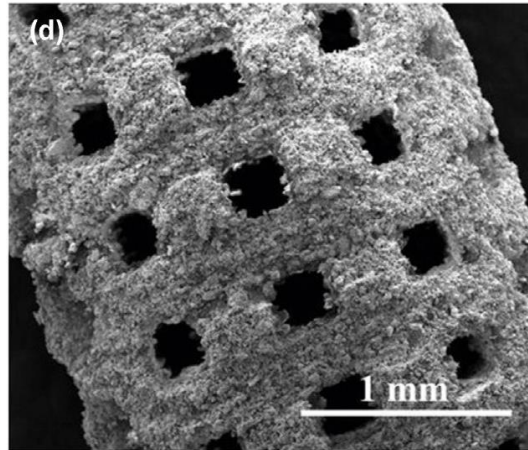
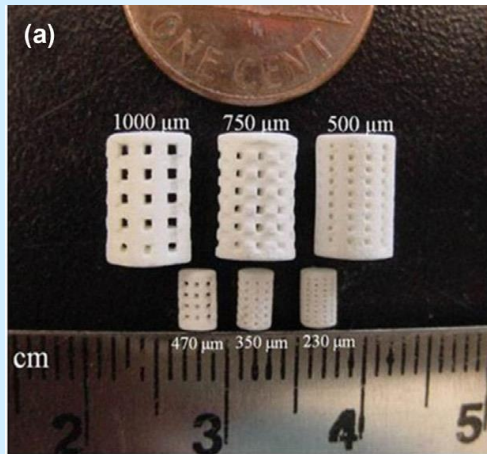
Conventional 3D Printing (Layer-by-Layer fabrication)



Polymer



Metal



Bio Fabrication

<http://3dprinting.com/products/architecture/>

<http://www.3dsystems.com/>

Tarafder et al., J. Tissue Eng. Regen. Med, 2012

Khalyfa et al., J. Mater. Sci.:Mater. Med., 2007

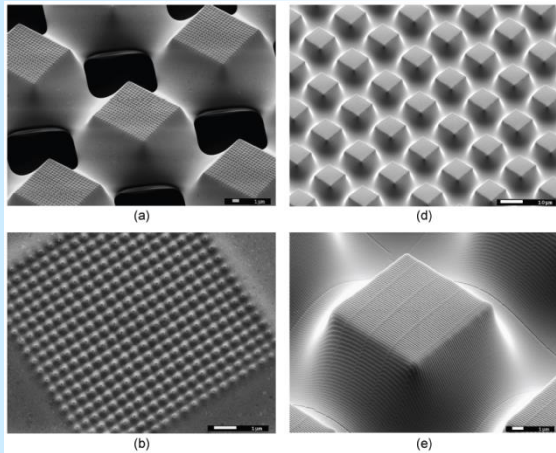
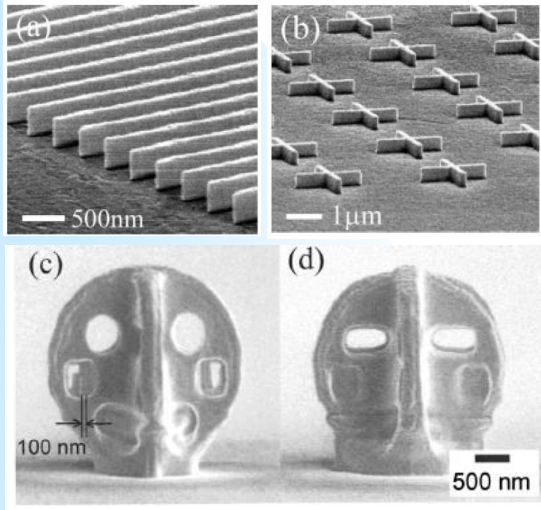


Seoul National University

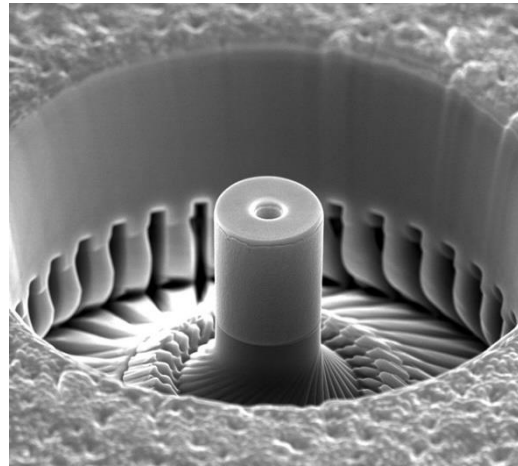
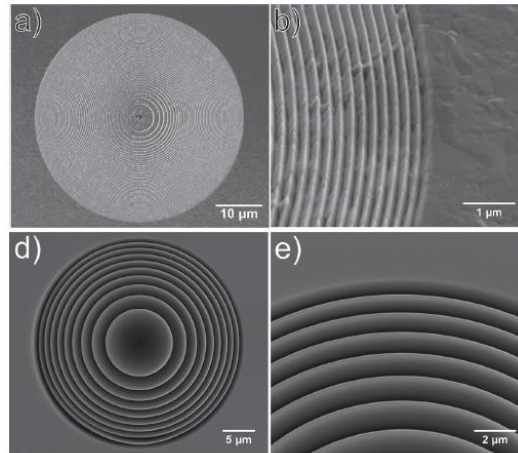
*Global Frontier Center
for Multiscale Energy Systems*

3D Nanofabrications

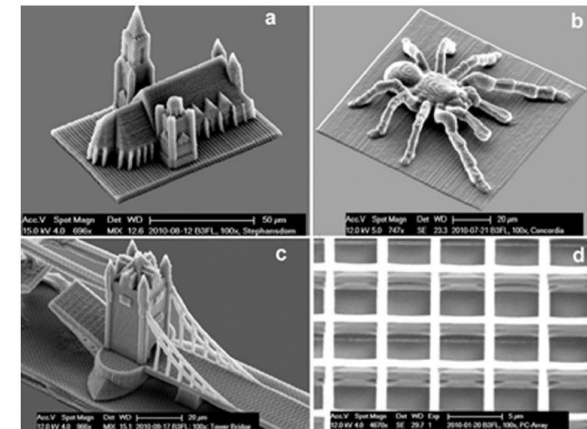
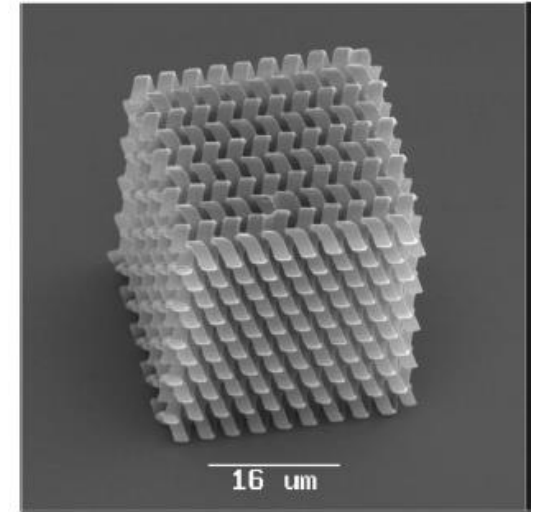
Electron beam lithography



FIB Lithography



Two-Photon Polymerization



Su et al., Adv.Mat., 2003

Yamaguchi et al., J. Vac. Sci. Technol. B, 2008

Feng et al., Adv. Fucnt. Mater. 2011.

Kahraman et al., Adv. Optical Mater. 2014.

Li et al. J. Polym. Sci. A Polym. Chem., 2011

Ovsianikov et al., ACS Nano, 2008

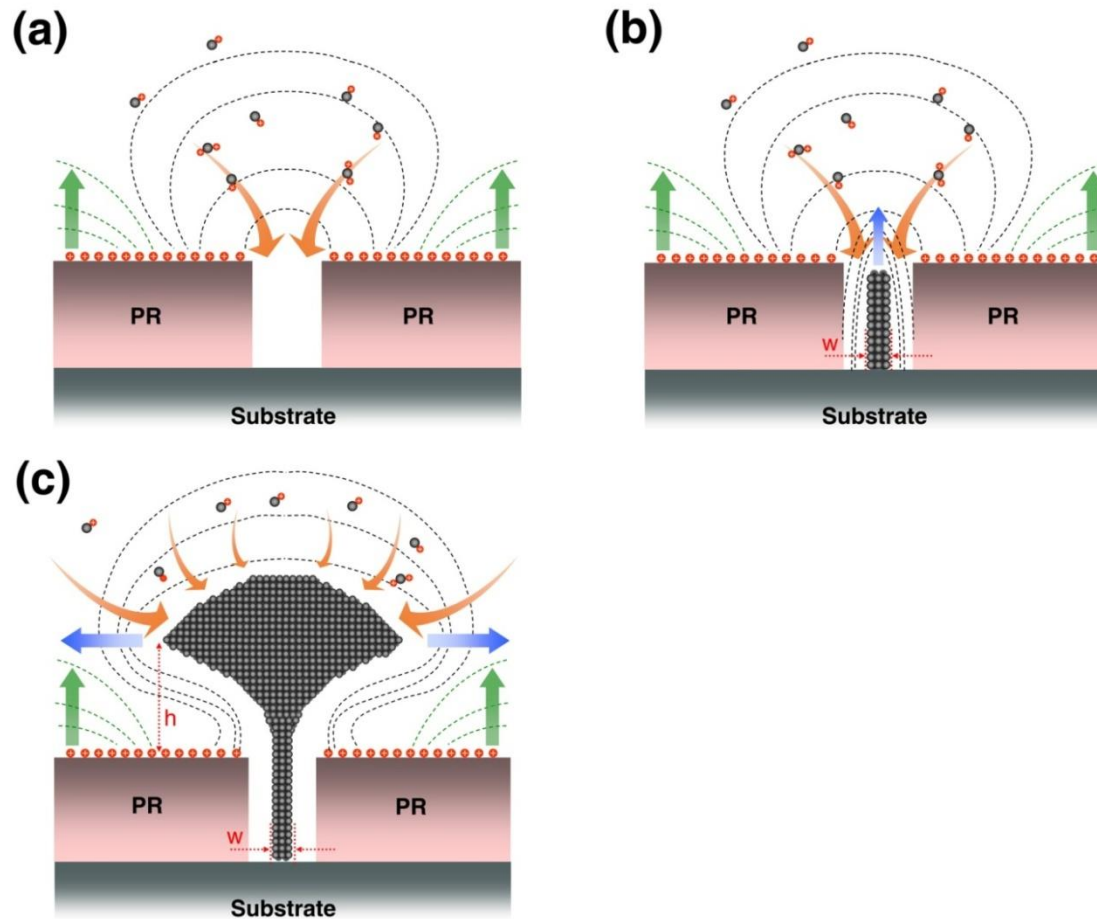
Seoul National University
Global Frontier Center
for Multiscale Energy Systems

Need to develop Cost-effective High-throughput 3D Nano-Assembly Technique:

**Multiscale, multidimensional assembly, Parallel,
Atmospheric, Nanoscale resolution, Large surface
area, Independent of substrates and materials**



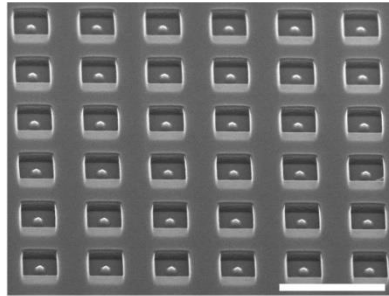
Scheme for 3D Assembly of Nanoparticles



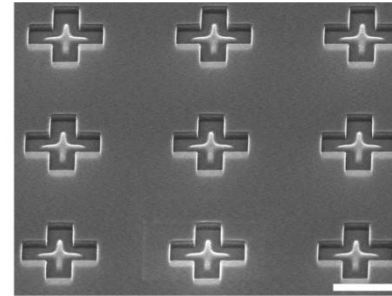
Time Dependent Growth of 3D Nanoparticle Structures Arrays

(Presented at 2008 AAAR Conference , Orlando, Abstract book, 2D. 04.)

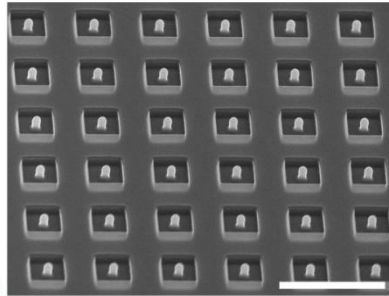
T=4 min



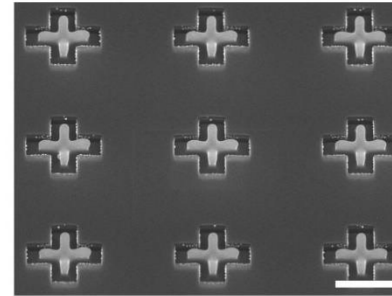
T=10 min



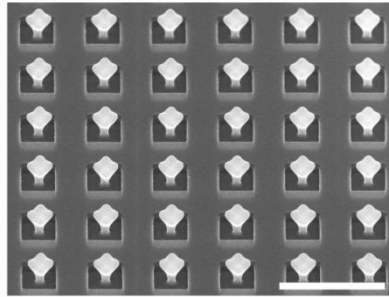
T=10 min



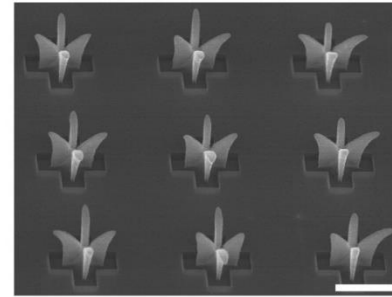
T=20 min



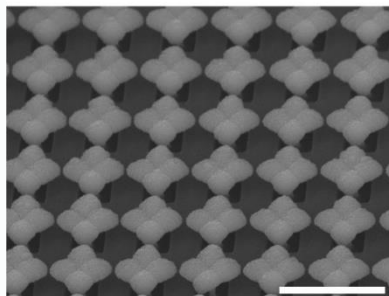
T=40 min



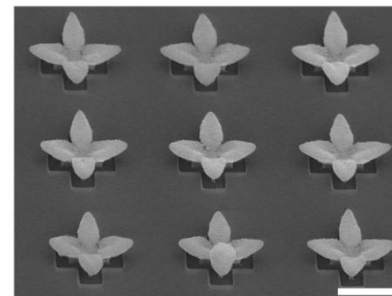
T=90 min



T=90 min



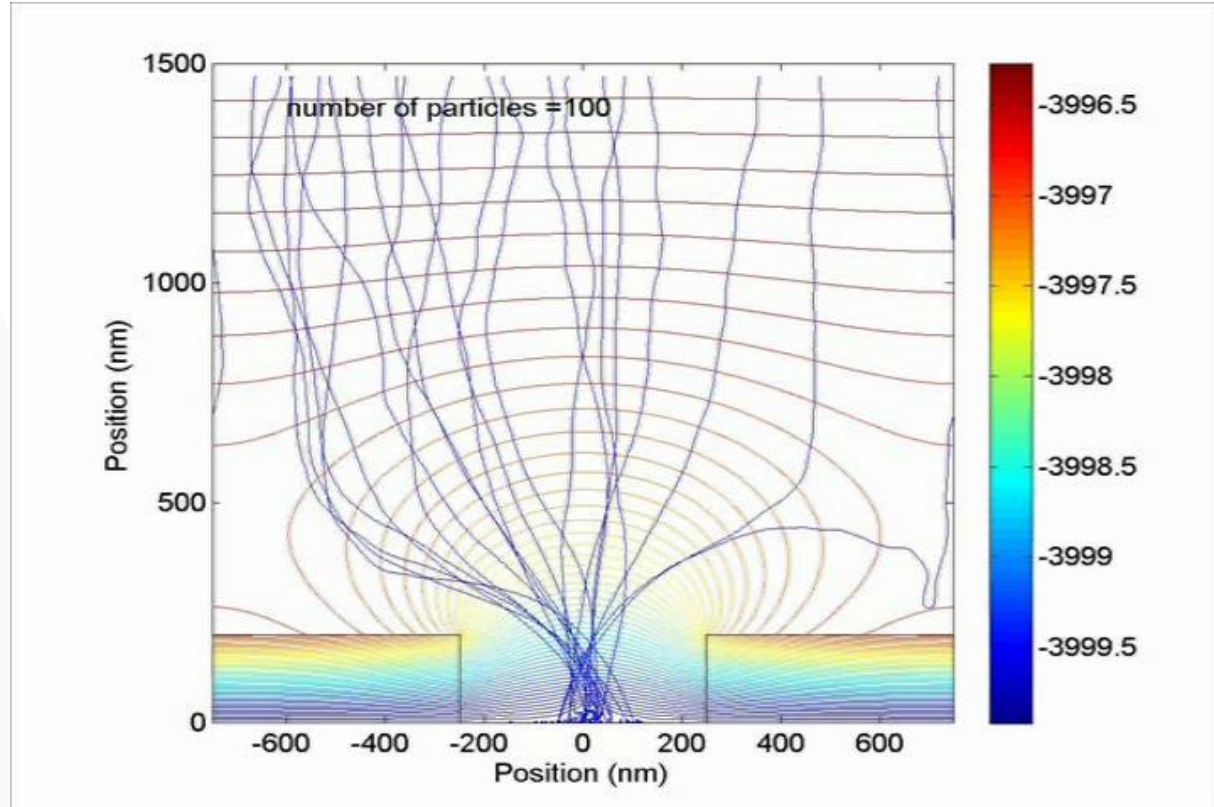
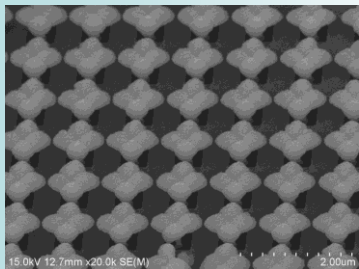
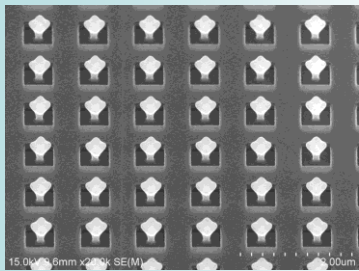
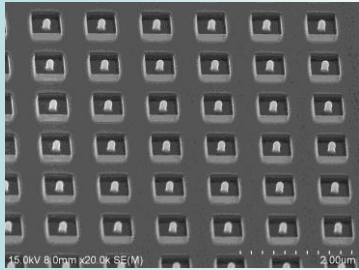
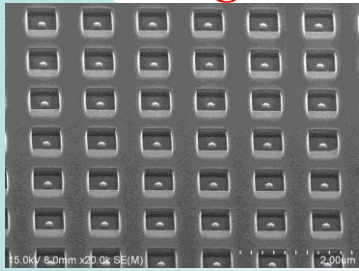
T=120 min



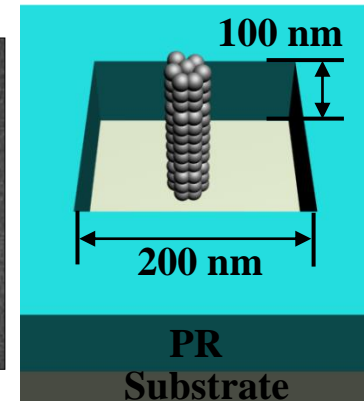
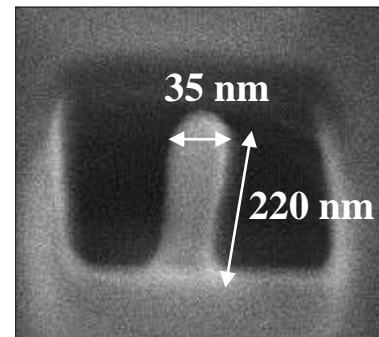
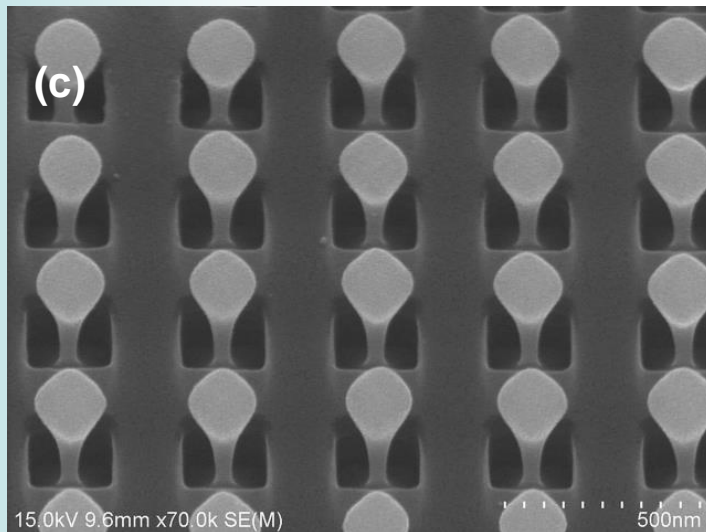
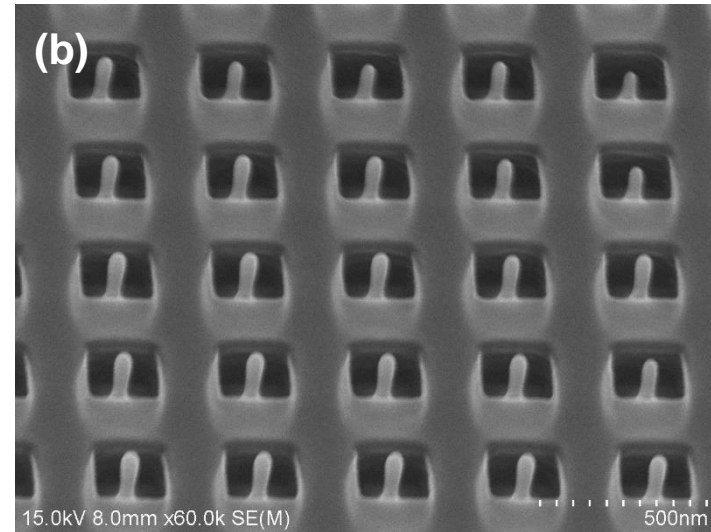
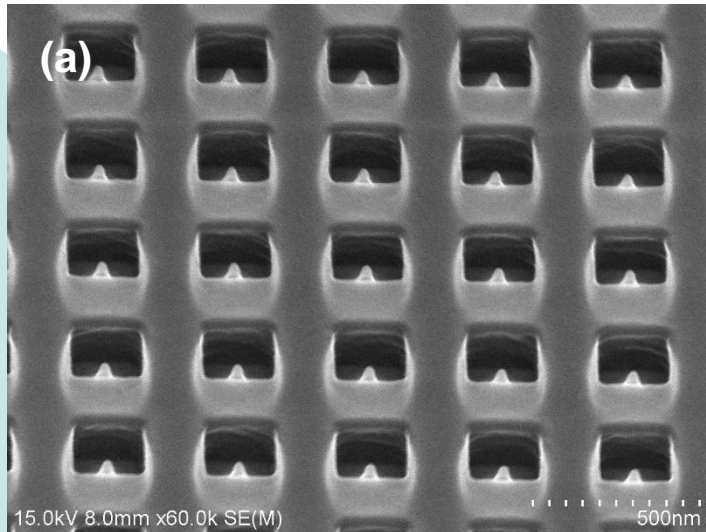
Scale bar : 1.5 μm

Growth of Nanoparticle Structure

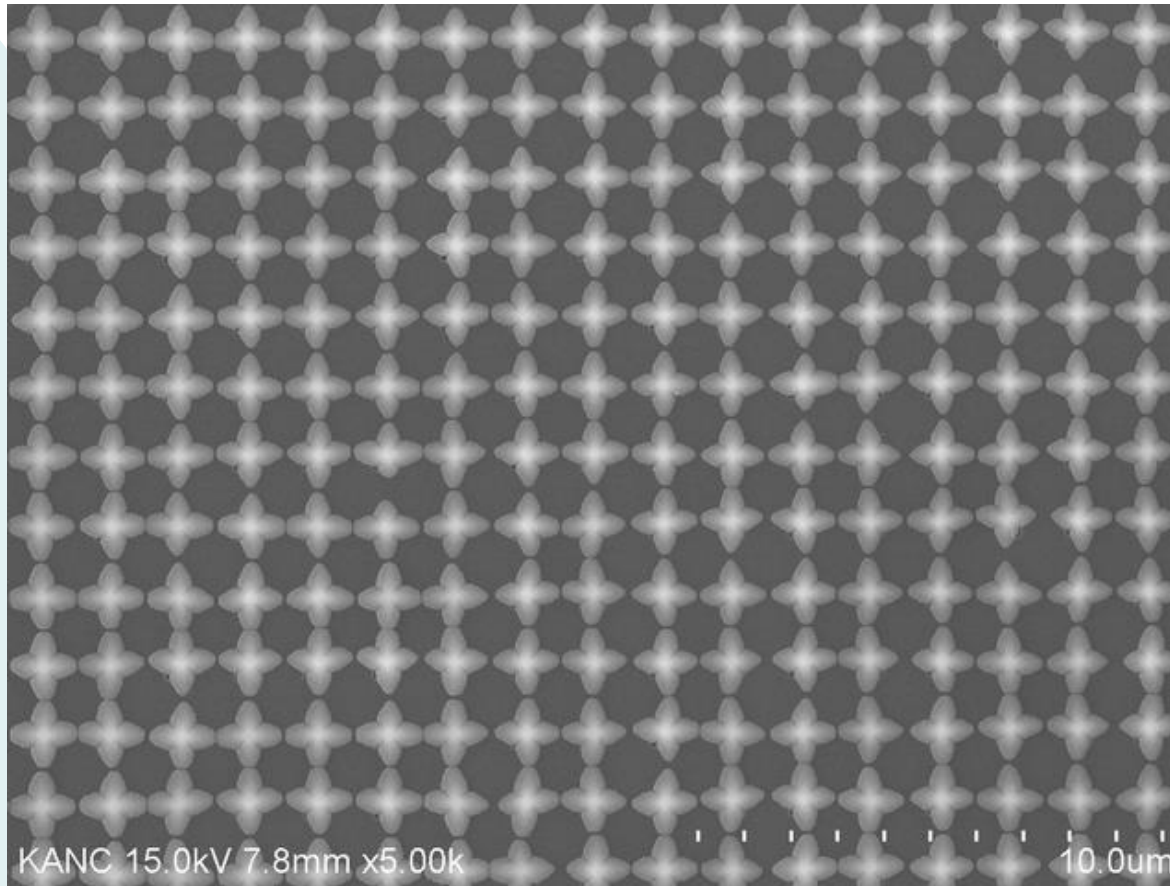
(Nano Letters, "Three dimensional assembly of nanoparticles from charged aerosols", Vol.11, 119, 2011)

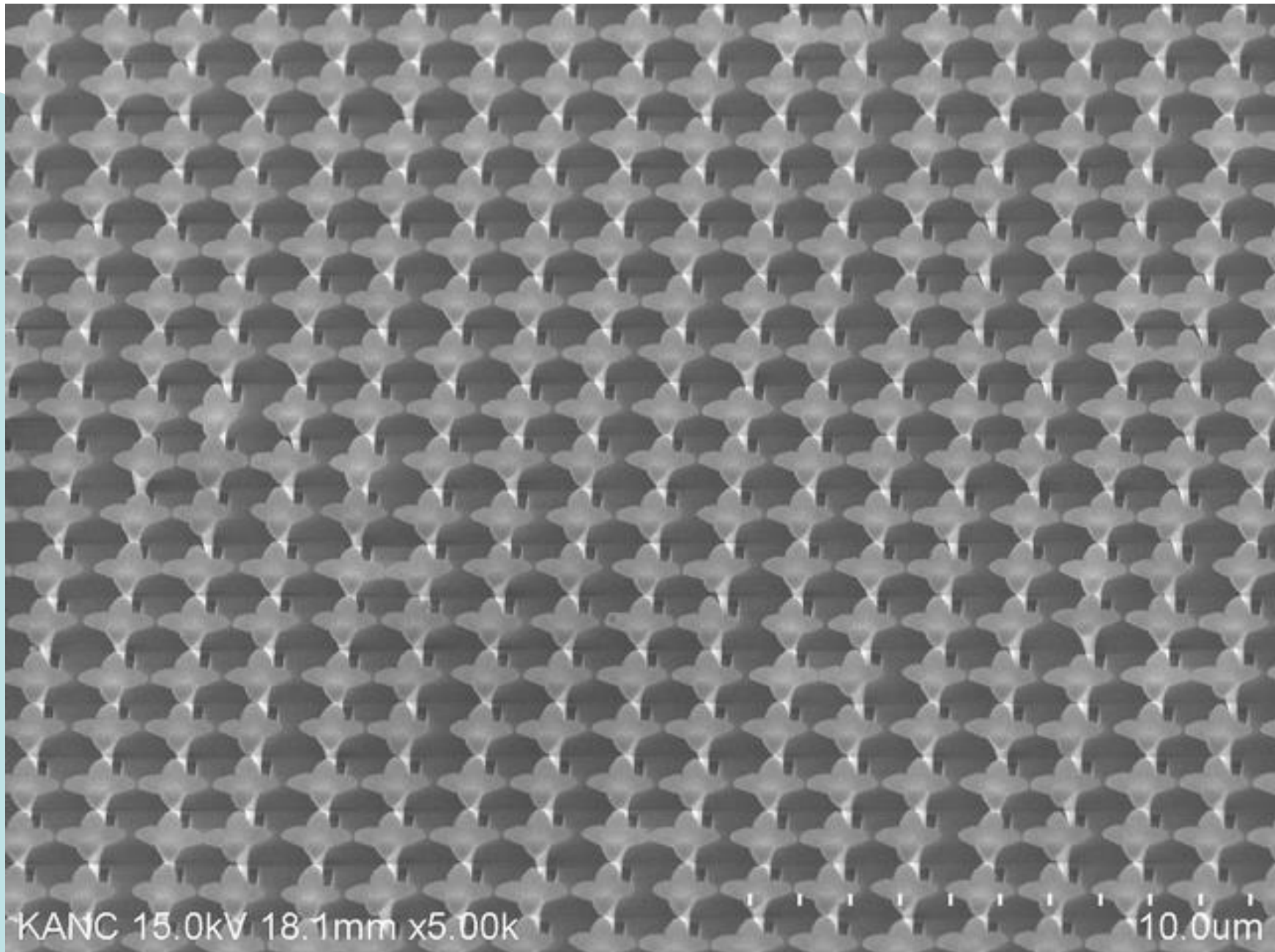


Array of 3D nanostructure of nanoparticles

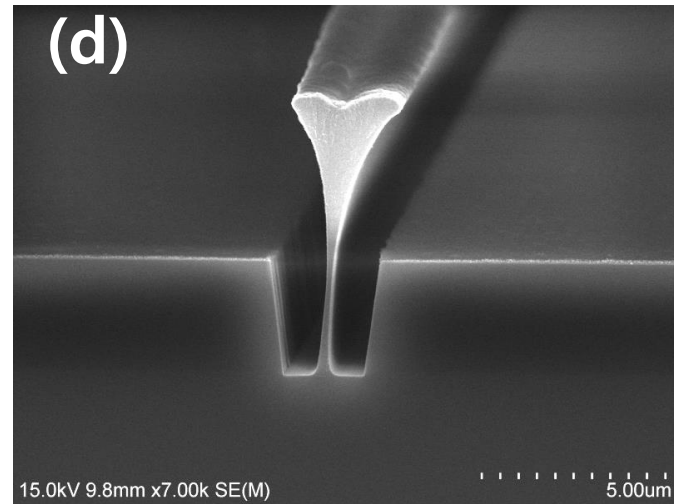
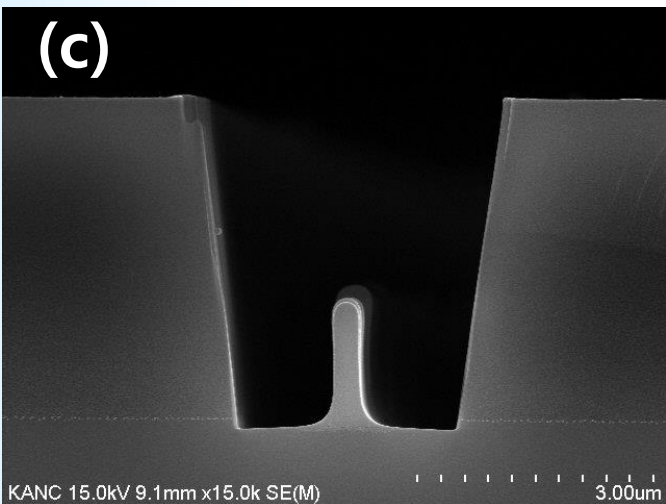
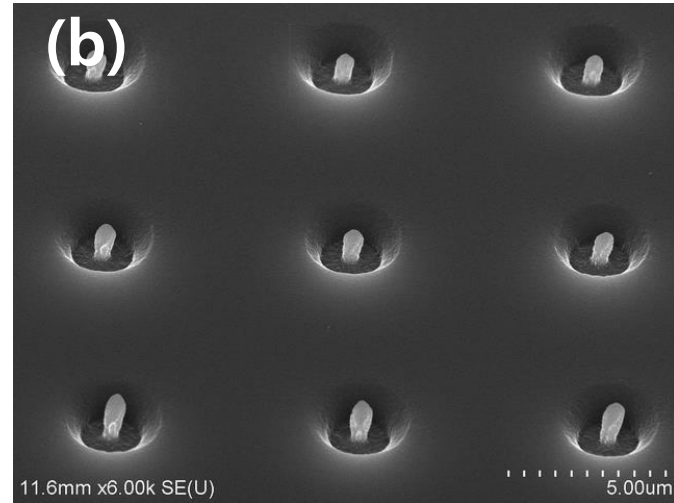
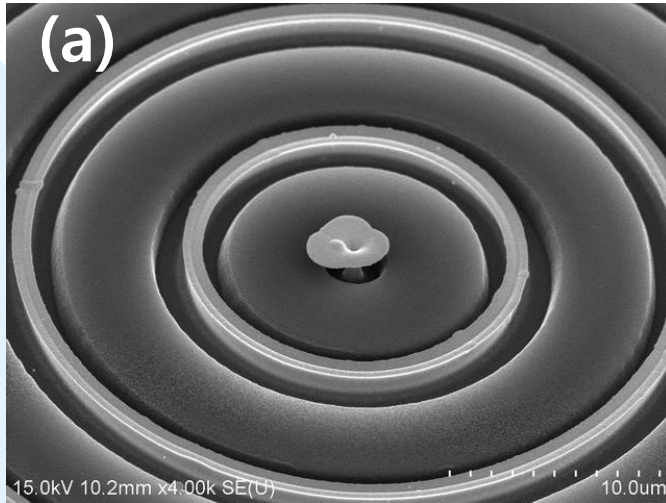


Four-leaf clover like 3D nanostructure array of nanoparticles (*Nano Letters*, vol. 11, 119)



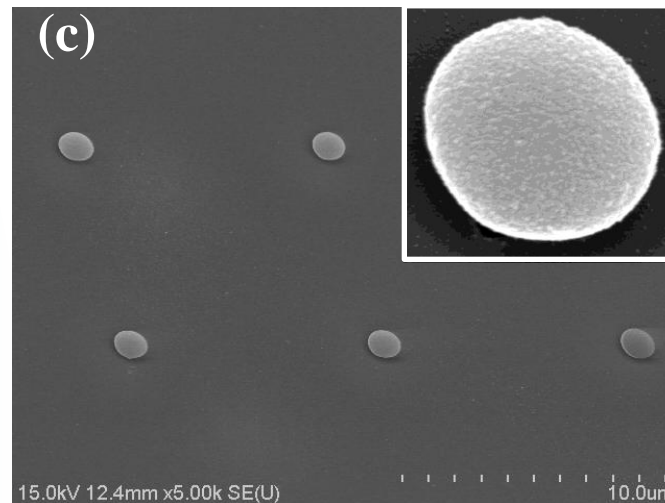
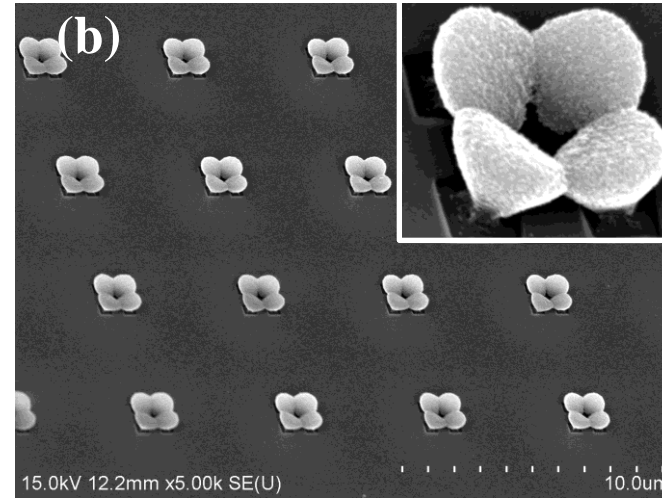
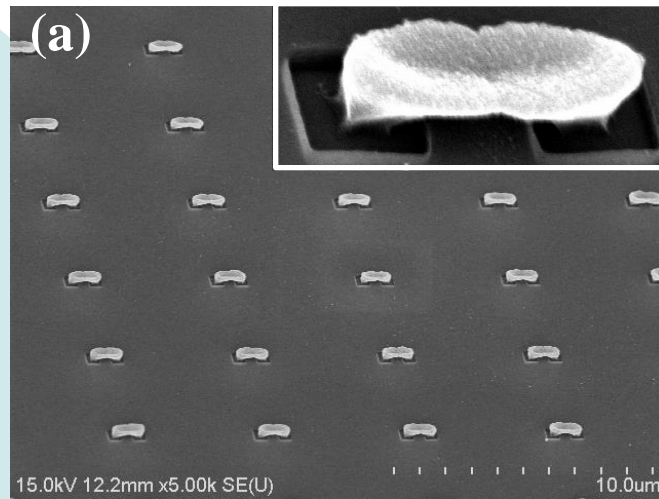


3D Nanoparticle Structures within Micron Scale SiO_2 Patterns (2008 AAAR Conference, Orlando)



Asymmetric assembly of nanoparticles

(Nano Letters, 2011)

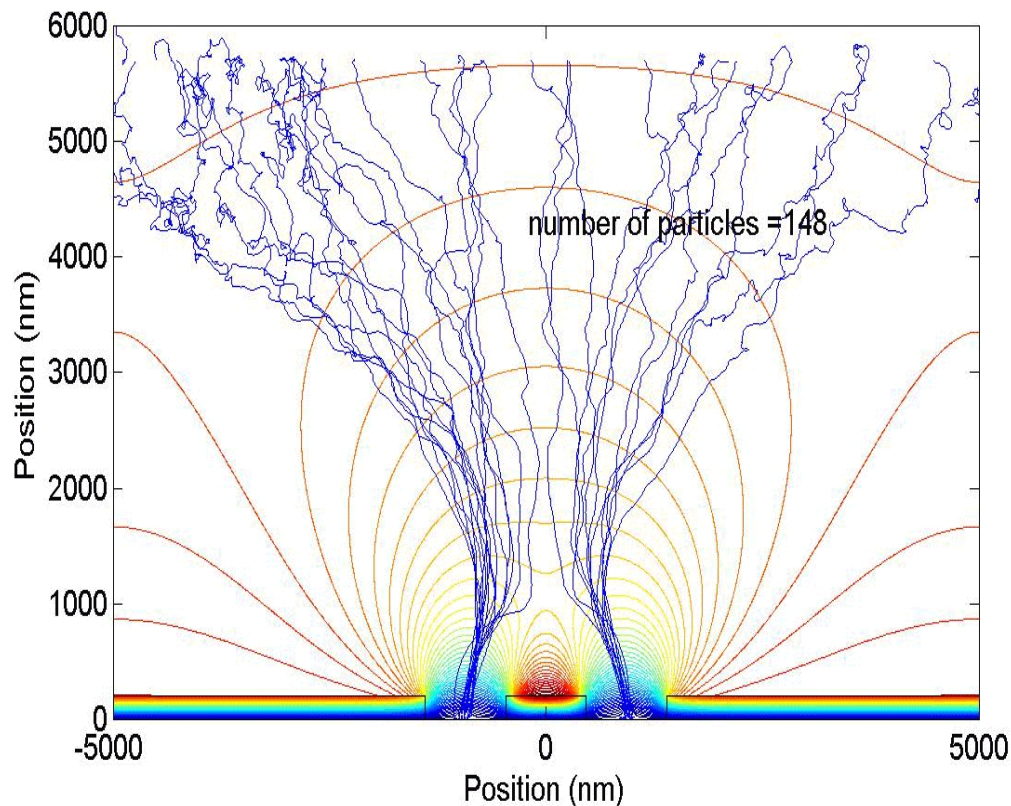
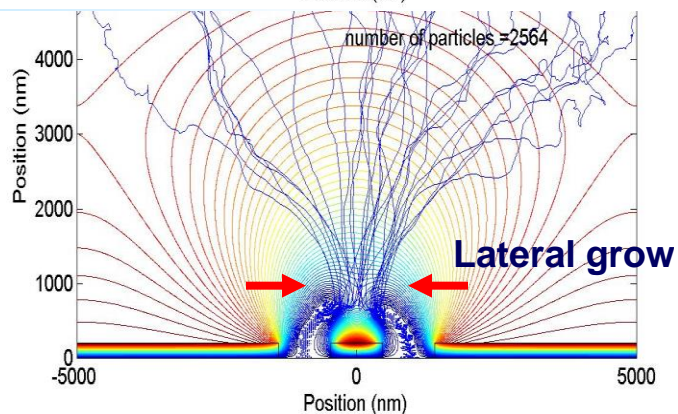
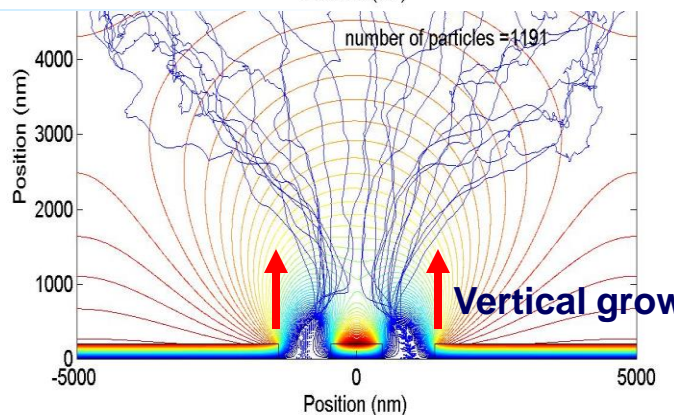
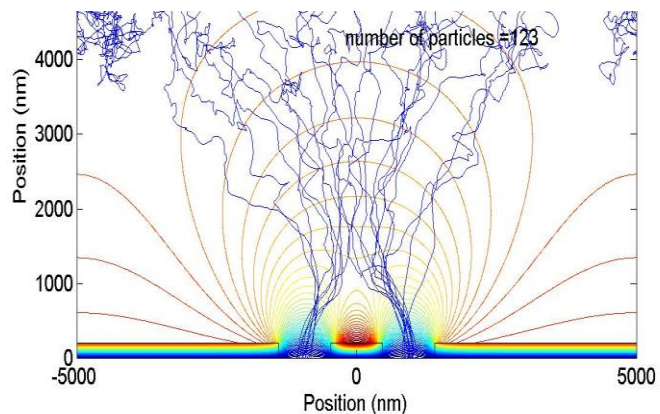


Pattern width : 500 nm



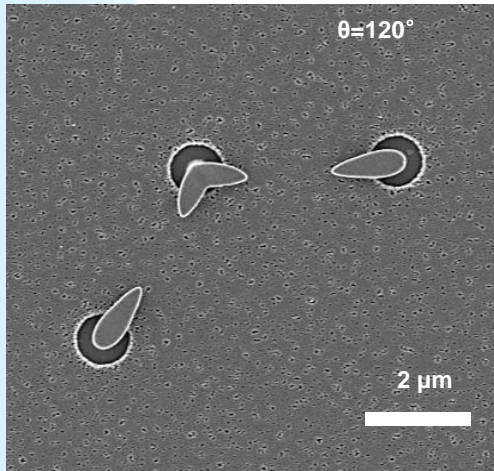
Seoul National University
Global Frontier Center
for Multiscale Energy Systems

Numerical simulation for asymmetric assembly of nanoparticles



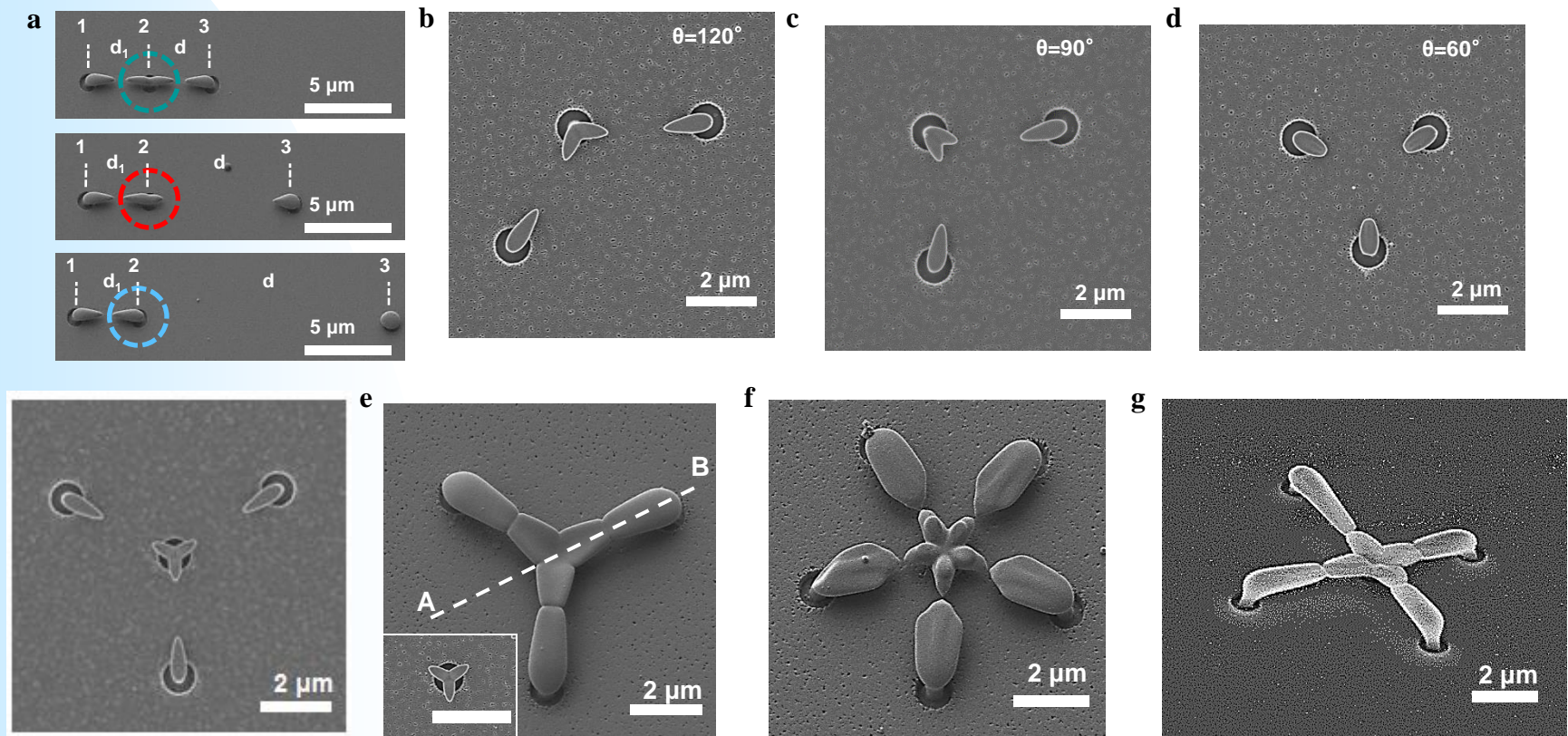
Bifurcation assembly of charged aerosols

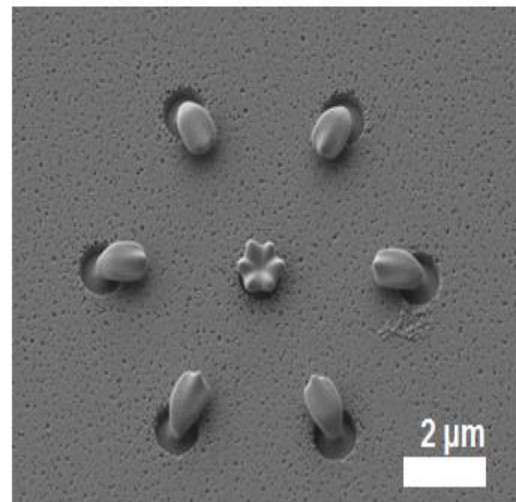
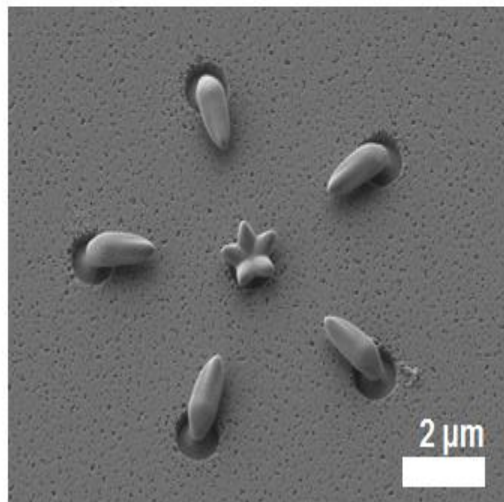
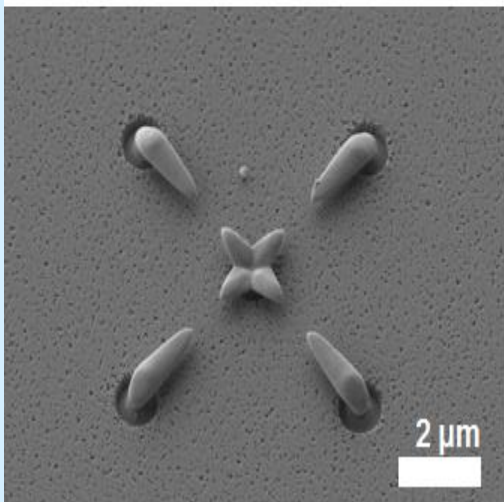
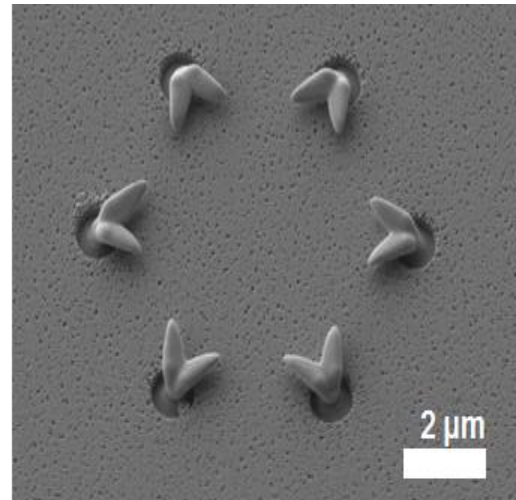
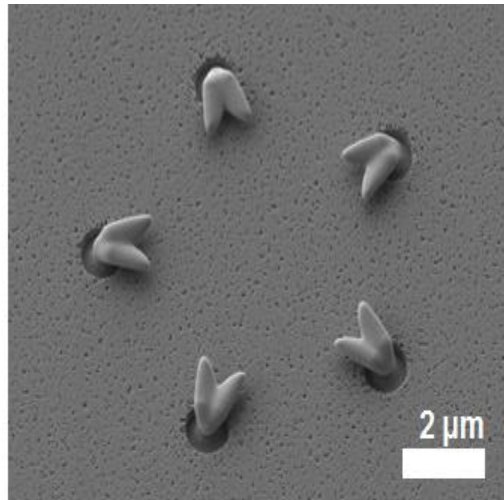
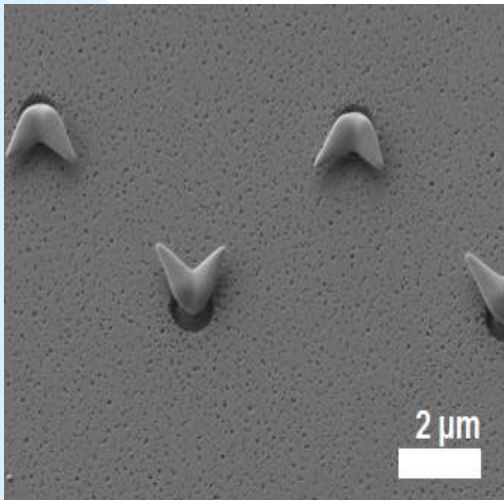
(Advanced Materials, 2017)



Multifurcation assembly of nanoparticles

(to be submitted)

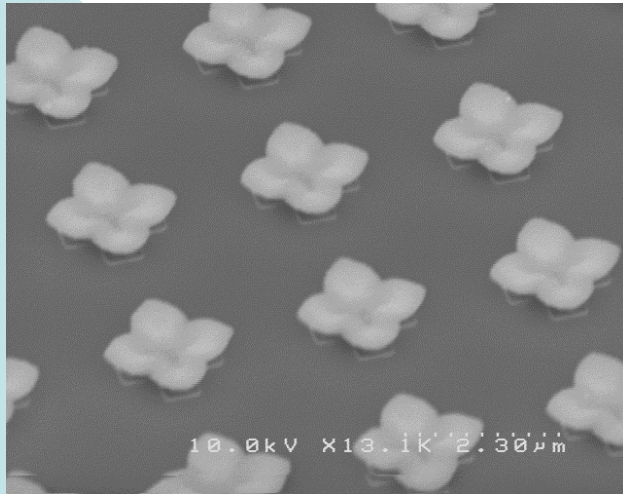




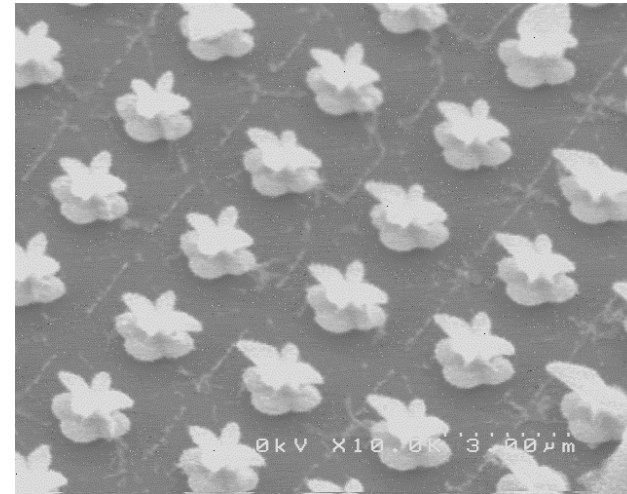
Multi-level 3D nanoparticle structure

(Nanotechnology, 2017)

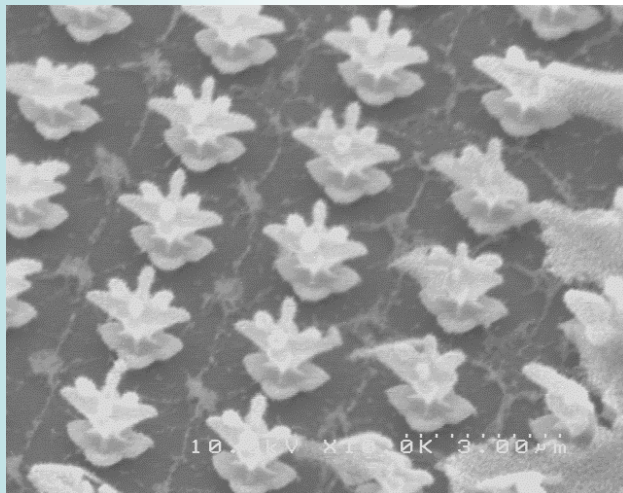
single-level



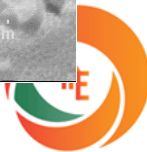
bi-level



tri-level

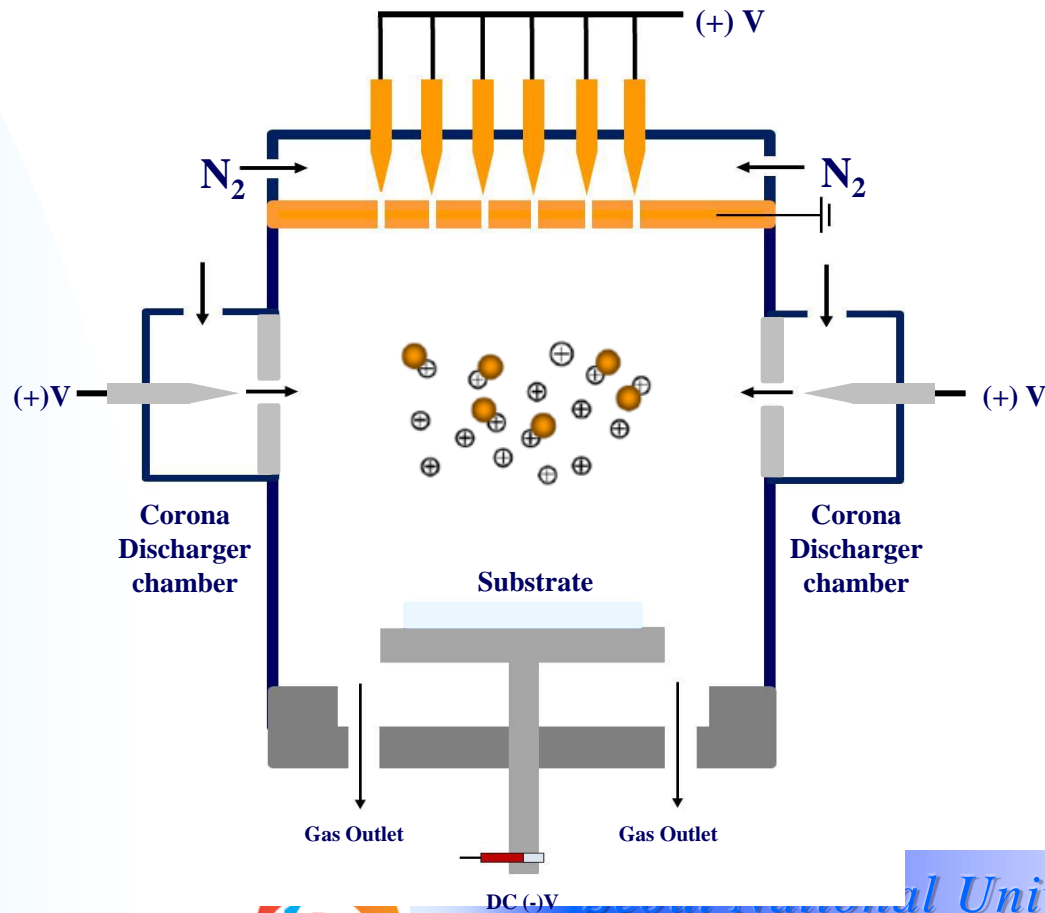


*Hydrangea:
Having multi-level
flower petals*

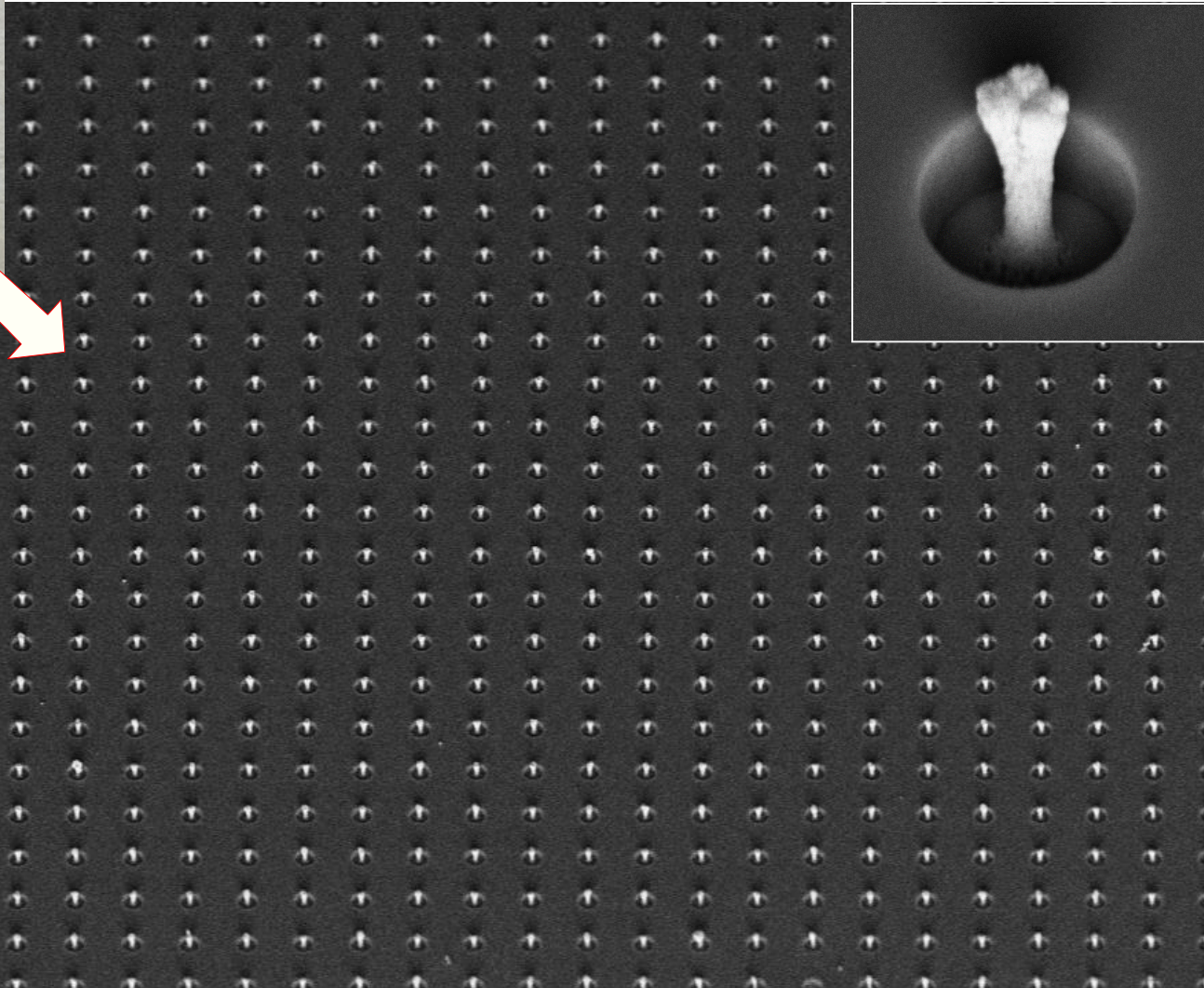
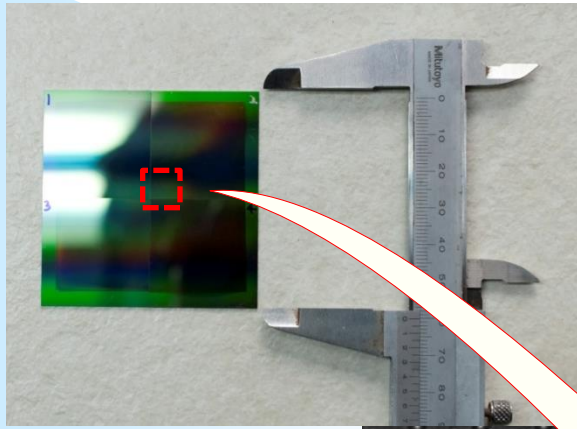


Large area 3D assembly based on multi-tip Spark-Discharge

(Nanotechnology, 2014)



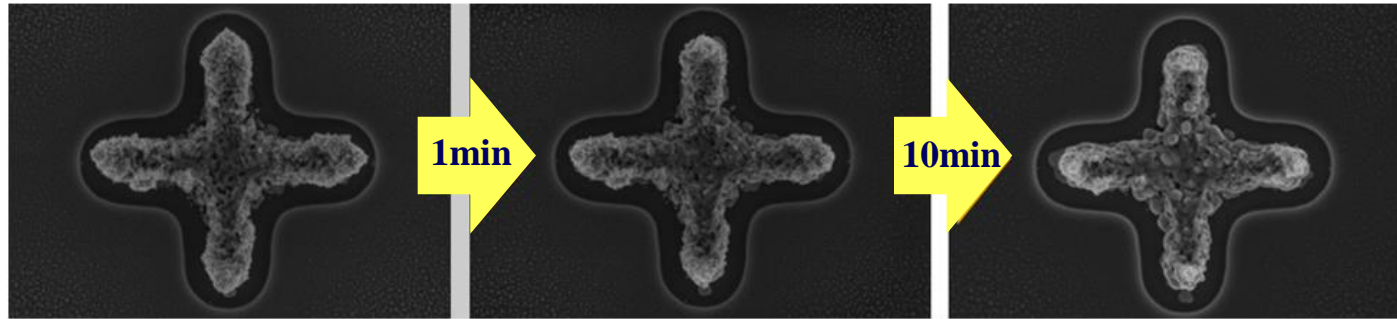
Large-area patterning (5cm X 5cm)



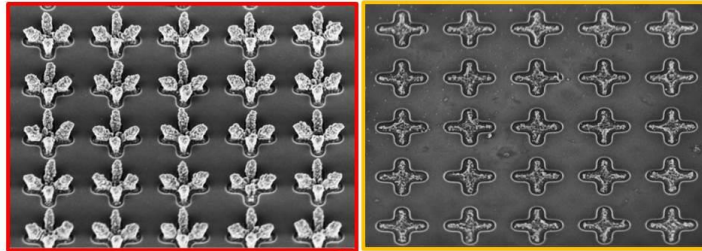
Mag = 2.00 K X 10 μ m WD = 8.6 mm EHT = 5.00 kV Signal A = InLens Contrast = 34.2% Date :13 Jan 2012 Time :17:28:33
SUPRA 55VP 31-04 Noise Reduction = Line Avg Brightness = 49.1% Chamber Status = Pumping (HV)

- Enhancement of mechanical strength of the 3D nanostructure by E-beam irradiation

E-beam annealing process



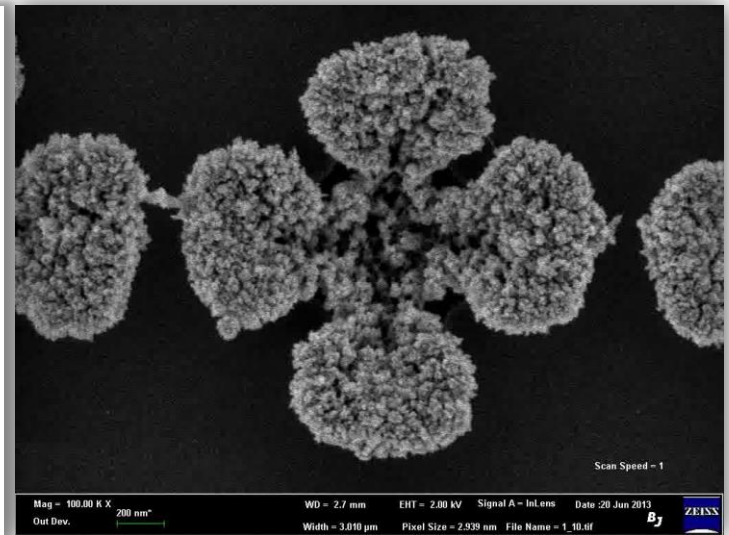
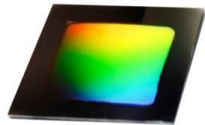
Increased mechanical hardness of nanostructures



3D nanostructure

E-beam irradiation

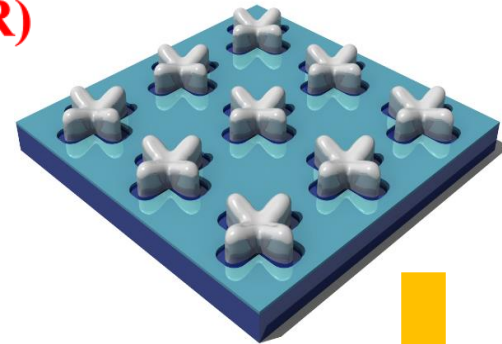
After sonication



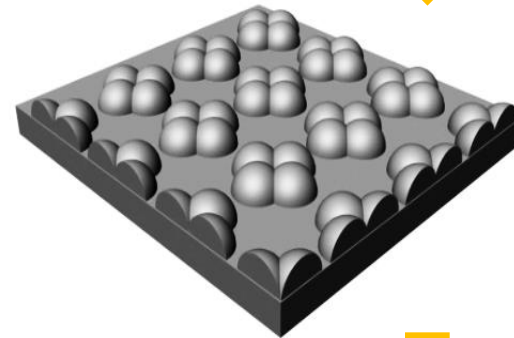
Si thin-film solar cell employing aerosol assembled 3D arrays.

: collaboration with Dr. Joonsik Cho (KIER)

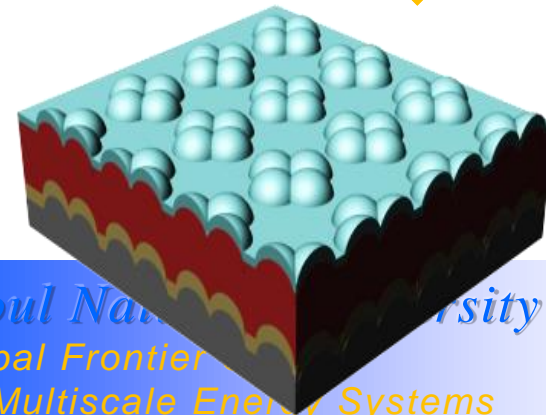
[1] Fabrication of 3D NPSs via ion assisted aerosol lithography (IAAL) with a multi-pin spark discharge generator



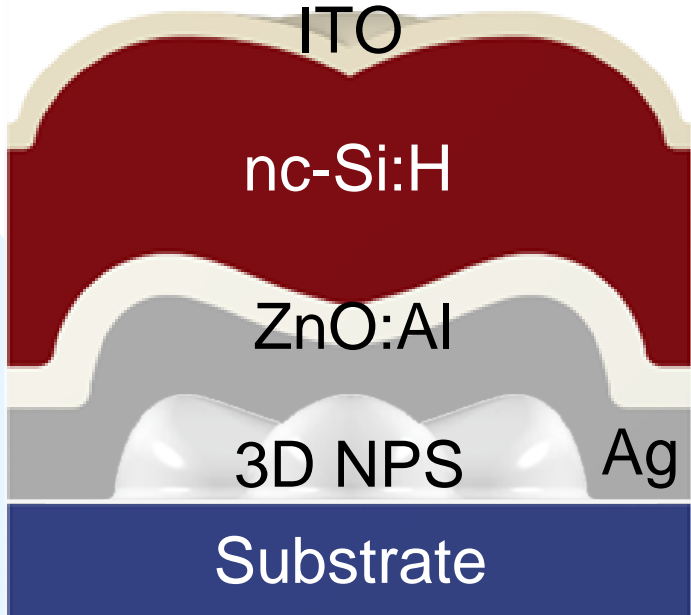
[2] Fabrication of 3D back reflectors by Ag deposition (Thermal evaporator)



[3] Fabrication of nc-Si:H thin-film solar cells by ZnO:Al (sputter), nc-Si:H (n-i-p configuration, PECVD), and ITO (sputter) deposition

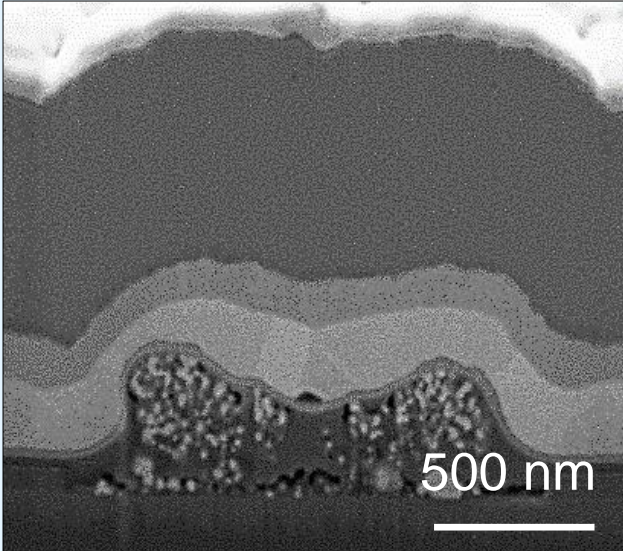


Device structure

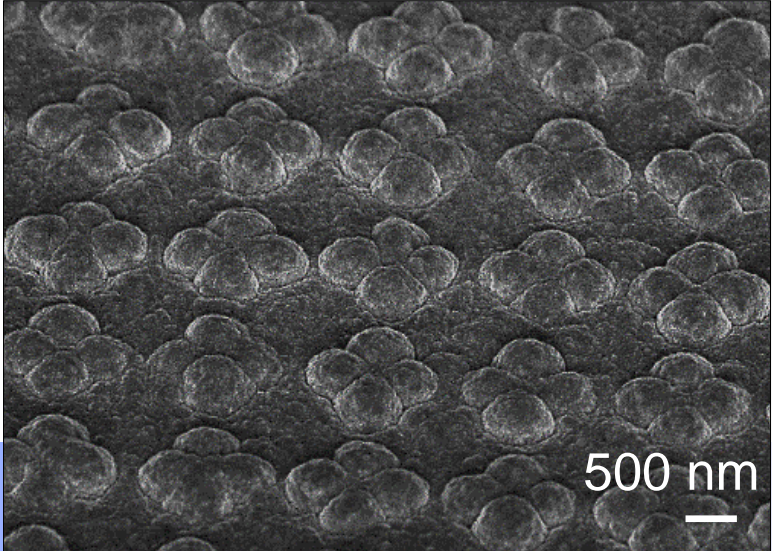


nc-Si:H thin-film solar cells
incorporating 3D nanoparticle structures (NPSs)

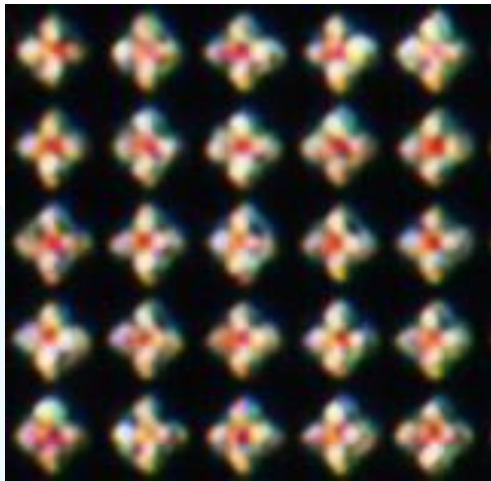
Cross-sectional view



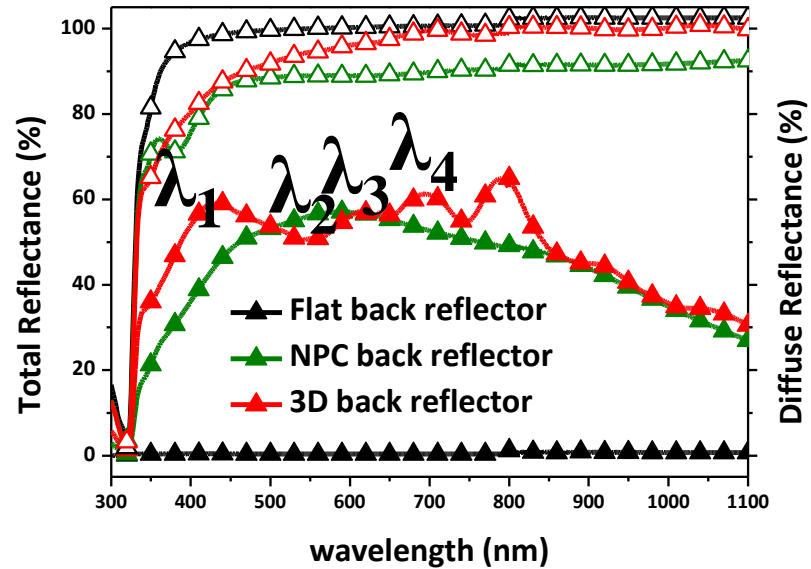
Tilted view



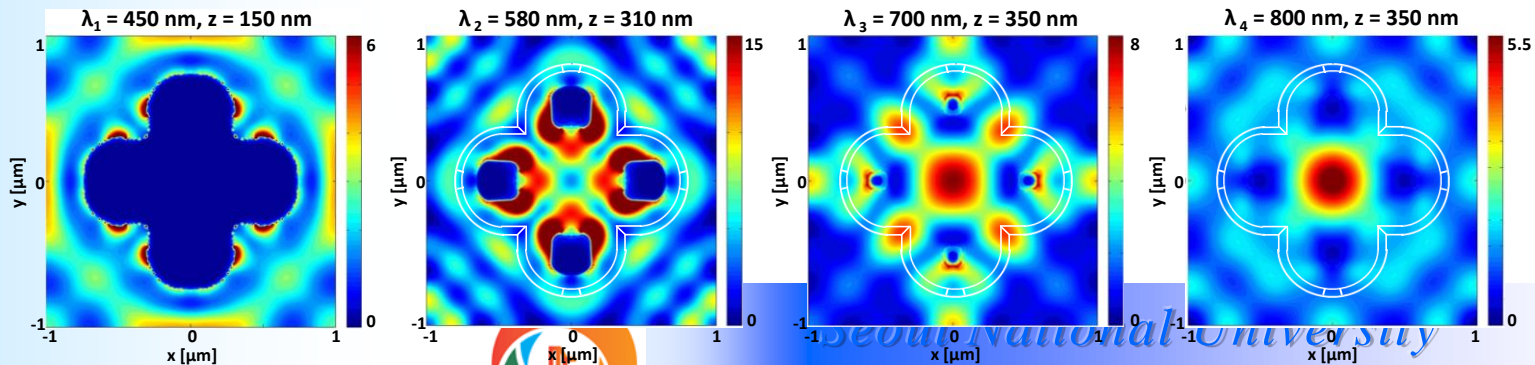
Multiple plasmon resonances of 3D back reflectors



Dark-field image
Multiple colors

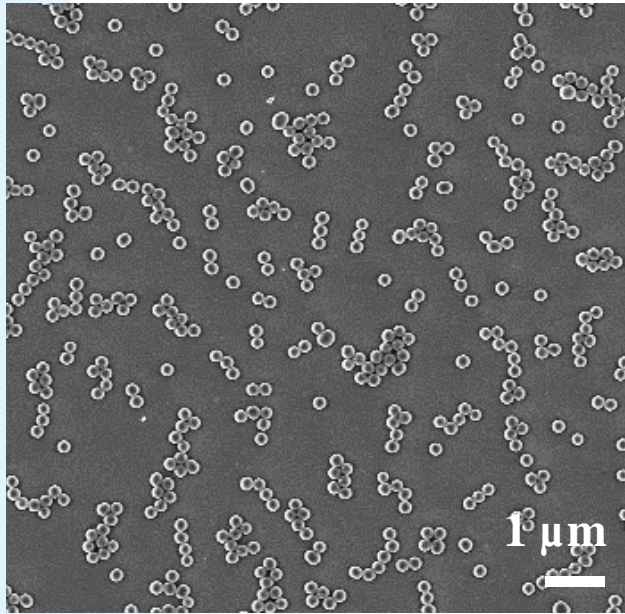


Localized electric field intensity profiles of the 3D back reflector at the multiple peaks



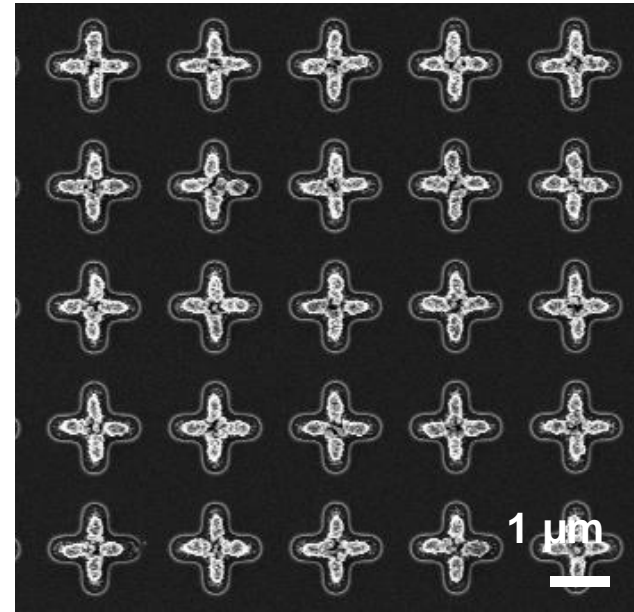
Comparison between random nanoparticle deposition case and 3D assembled structure case

(Nanotechnology, 27, 055403, 2016)



Nanoparticle clusters (NPCs)

VS



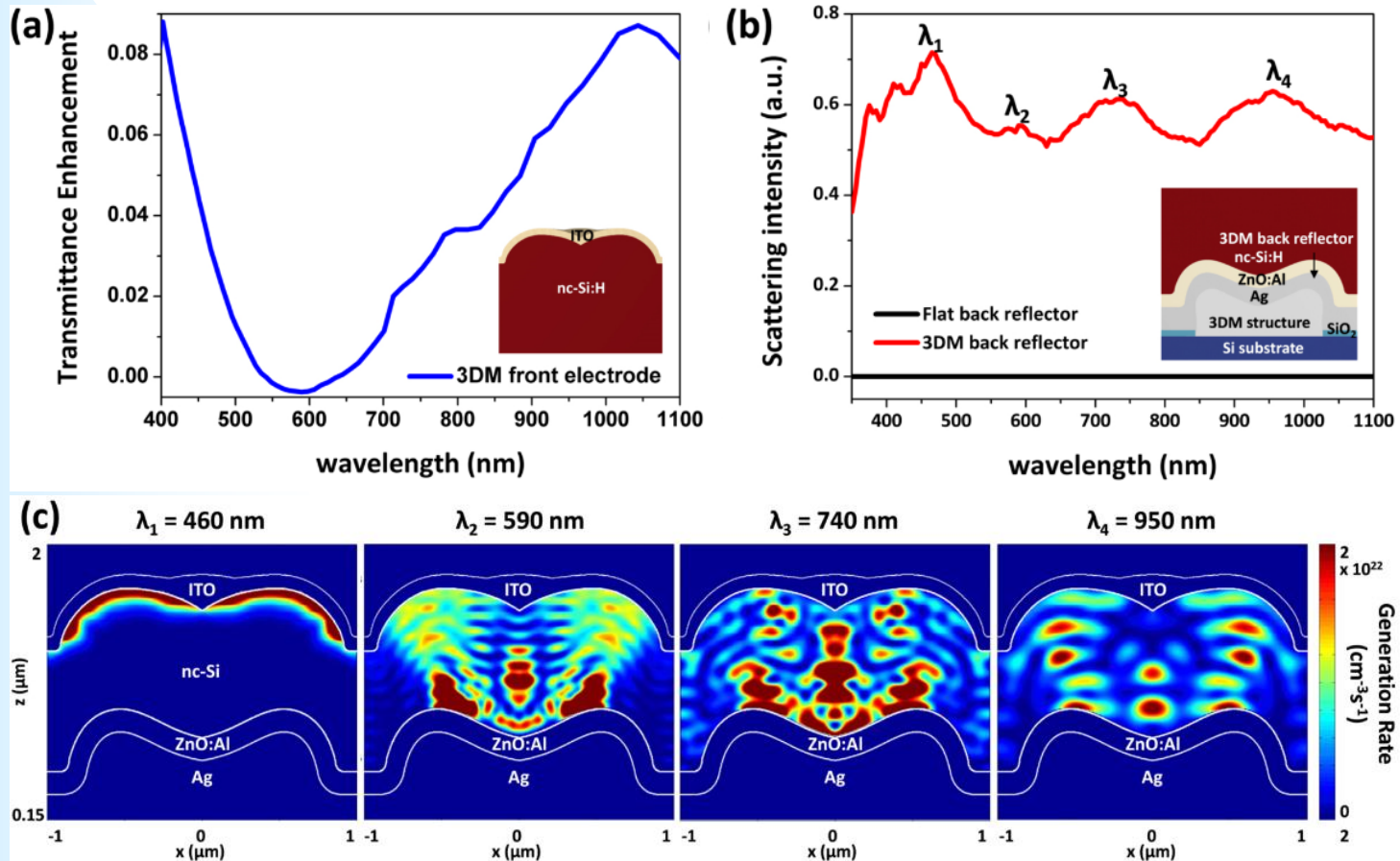
3D NPSs

Same surface coverage: 12%

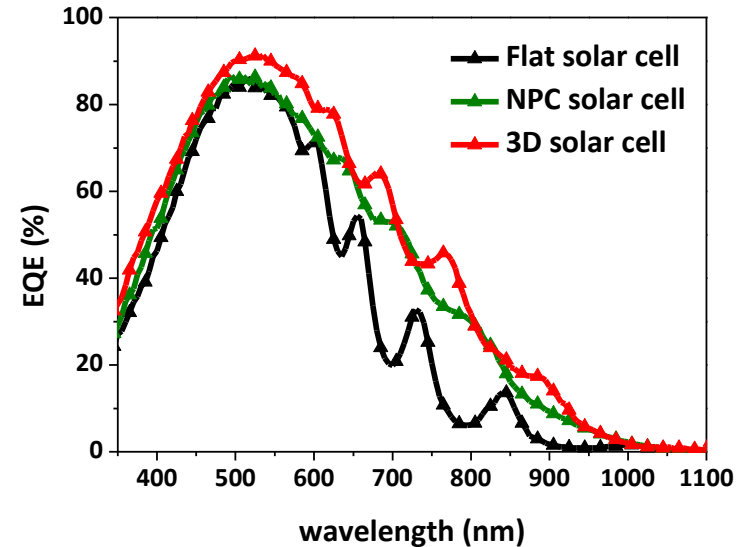
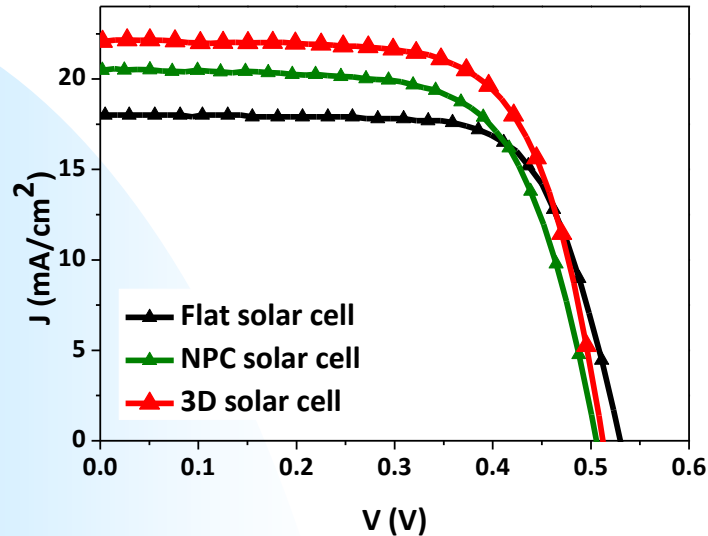


Multiple plasmon resonances: Simulations

Nanocrystalline silicon thin-film solar cells using 3D nanostructures
(*Nanotechnology*, 27, 055403, 2016)



Enhanced performance of 3D solar cells



	V_{oc} (V)	J_{sc} (mA/cm ²)	FF (%)	Efficiency (%)
Flat solar cell	0.53	17.05	70.97	6.41
NPC solar cell	0.51	20.48	67.46	6.98
3D solar cell	0.51	22.07	68.71	7.77

